Investigation of the Energy Recovery from Potential Industrial Processing Using Thermoelectric Generator Devices (TEG) And Process Control System

By

PAUL EGHOSA OROBOR

PG/ENG1407007

A PROJECT REPORT SUBMITTED TO THE DEPARTMENT OF MECHANICAL ENGINEERING, FACULTY OF ENGINEERING, UNIVERSITY OF BENIN CITY IN PARTIAL FULFILLMENT OF THE REQUIREMENT FOR THE AWARD OF A MASTER OF ENGINEERING DEGREE

March, 2025

DECLARATION / CERTIFICATION

This is to certify that this work on Investigation of the Energy Recovery from Potential Industrial Processing Using Thermoelectric Generator Devices (TEG) and Process Control System was carried out by PAUL EGHOSA OROBOR (PG/ENG1407007) in the Department of Mechanical Engineering, Faculty of Engineering, University of Benin, Benin City.

__________________________ __________________________

Dr. H.O. Egware *Date*
Supervisor

__________________________ __________________________

Prof. O.O. Ighadaro *Date*
Head of department

DEDICATION

This project is dedicated to my family, Mrs. F. G. Orobor, Joseph, Paullet, Aisosa, Jessica, and Jennifer Orobor and most especially to my late father, Dr. N. P. Orobor, whose words had a profound impact on my life. His encouragement and guidance continued to inspire me to work hard when he was alive, and his memory still motivates me never to give up.

ACKNOWLEDGEMENTS

I would like to express my profound gratitude to my supervisor, Dr. H.O. Egware, for his dedicated guidance, encouragement, and invaluable support throughout the course of this project. I also extend my sincere appreciation to Engr. P. O. Olagbegi, Engr. Dr. O. J. Unuareokpa, Prof. G. O. Ariavie, Prof. E. G. Sadjere, and Prof. A. I. Obanor for their professional assistance, supportive advice, and driven motivation, which greatly contributed to the success of this research work.

Special gratitude to the Head of Department, Prof. O.O. Ighadaro, for his helpful suggestions and emotional support. I appreciate my colleagues and friends in the Department of Mechanical Engineering for their contribution to the success of this project.

My heartfelt appreciation also goes to my beloved mother, Mrs. F. G. Orobor, whose unwavering love, prayers, and guidance have been my greatest source of strength and inspiration. I am equally grateful to the almighty God for everything

ABSTRACT

Most industrial heat exchanger devices, such as condensers, boilers, furnaces, and pipelines generate a certain amount of heat waste due to temperature gradient in the fluid. Leading to reduction of the efficiency, increased emissions, and higher fuel consumption. Thermoelectric generator (TEG) technology offers a sustainable solution by utilising the waste heat to generate electricity. This project focuses on the performance of the TEG process using the counter-flow heat exchanger and process control mechanism to monitor the results evaluated from the different thermal transfer conditions. The primary objective is to recover electricity from heat waste from industrial pipelines or heat exchanger devices, and to assess the feasibility and predict the performance of TEG for sustainable power generation.

The experiment components are aluminium heat exchanger tubes, thermal paste, TEG modules (SP1848-27145), thermal paste, Arudino, Voltage and Current sensor, 16X2 LCD display, and Multimeter. The setup of the experiment utilised two aluminium heat tubes: the upper tubes flowed with Hot water, while the lower part circulated with cooling water. The five series modules were mounted between the surfaces of both heat exchanger tubes using thermal paste to ensure heat transfer. The reading of the voltage and current values was displayed using a 16X2 LCD with Arduino Nano or a Multimeter.

Experimental results show that the system successfully converted a measurable fraction of waste heat into electrical energy. While the power output and efficiency were relatively low compared to the total heat transfer across the exchanger tubes, the system achieved a maximum output of 9.28 V and 3.17 W, with an efficiency of 14.5%. Based on the empirical model, 5000 thermoelectric modules (TEMs) could generate a maximum power output of 3.17 kW when properly installed, which can improve the overall efficiency in the industrial application.

TABLE OF CONTENTS

CHAPTER THREE: MATERIALS AND METHODS

CHAPTER FOUR: RESULT AND DISCUSSION

CHAPTER FIVE: CONCLUSION AND RECOMMENDATION

LIST OF FIGURES

LIST OF TABLES

NOMENCLATURE

Abbreviation

DCS	distributed control systems
HXR	heat exchanger
LMTD	Logarithmic Mean Temperature Difference
TEM	thermoelectric module
TEG	thermoelectric generator
TIM	thermal interface materials
PCS	process control system
PLC	programmable logic controller
WHR	waste heat recovery
SCADA	supervisory control and data acquisition (Acronym)

Subscripts

c	*cold body or fluid*
e	exit
h	*hot body or fluid*
i	inlet
I	inner
M	mean

o outer

p constant pressure

ci cold fluid at the inlet

ce cold fluid at the exit

he hot fluid at the exit

hi hot fluid at the inlet

hn and cn hot and cold surface at the position of the nth of TEG.

$ambient$ parameter in air

Symbols

A	effective heat transfer area (m^2)
I	current (Amp or A)
K	Thermal conductivity (W/mK)
h	convective heat transfer coefficient (W/m^2)
ρ	Density (kg/m^3)
P	power (W)
r	radius of the pipe (m)
t	Time evolution(s)
T	Temperature at the different radial position (k)
V	voltage (V or Volt)
Q	heat transfer rate (W/s)
U	overall heat transfer coefficient ($W/m^2 \cdot K$)
c_p	Specific capacity of the fluid at constant pressure (kJ/kgK)
α	Seebeck co-efficient
ΔT	Temperature difference across the junction
$T_{ambient}$	Ambient temperature
$h_{ambient}$	Heat convection coefficient of air
D_O	Outer diameter of the tube or pipe
D_I	inner diameter of the tube or pipe

θ_M	log mean temperature difference (LMTD)
Q_h	heat transfer by the hot fluid (W/s)
$\dot{m}_h$	mass flow rate of the hot fluid (kg/s)
c_p	specific heat capacity of the fluid at a constant pressure(kJ/kgk)
T_{hi}	temperature of the hot fluid at the inlet (k)
T_{he}	temperature of the hot fluid at the exit (k)
Q_c	heat transfer by the cold fluid
$\dot{m}_c$	mass flow rate of the cold fluid
c_p	Specific heat capacity of the fluid at a constant pressure(kJ/kgk) (for water4.186~4.200 kJ/kgk or 4200 J/kgk)
R_L	Load resistance
T_{ci}	temperature of the cold fluid at the inlet (k)
T_{ce}	temperature of the cold fluid at the exit (k)
θ	temperature difference between the hot and cold fluids (K)
T_{hn}	the hot surface temperatures at the position of the nth of TEG.
T_{cn}	the cold surface temperatures at the position of the nth of TEG.
η	Efficiency of the system

CHAPTER ONE

INTRODUCTION

1.1 BACKGROUND OF STUDY

Industrial systems such as heat exchangers, boilers, condensers, turbines, and processing pipelines generate substantial waste heat during operation. In most industrial setups, this waste heat is lost to the atmosphere, leading to increased energy losses, wasted fuel, and higher operational costs. However, with the current global focus on energy efficiency, sustainability, and reduced emissions, the harnessing and reuse of industrial waste heat has become a significant area of interest for engineers. A new technology with the potential to solve this problem is the Thermoelectric Generator (TEG), which directly converts heat into electrical power using the Seebeck effect, without moving parts, noise, or combustion.

Although waste heat recovery using TEG systems has significant potential, the process also faces several challenges. The efficiency of thermoelectric energy conversion remains low, and maintaining a temperature gradient between the hot and cold junctions of the TEG is also difficult in an industrial setting. Previous studies have explored ways to improve thermoelectric performance, including the use of advanced semiconductor materials, with high performance of TEM values (Fei *et al.,* 2014), advanced heat sink designs to reduce thermal resistance and improve heat dissipation (li *et al*., 2021) and fluid-based cooling techniques incorporating Nano fluids or forced fluid systems to increase heat transfer efficiency.

However, there is still a critical research gap in this area that needs to be addressed: the experimental, controlled assessment of TEG performance on heat exchanger tubes, with a real-time process control system to optimise temperature difference and system stability. In many previous studies, there has been a lack of comprehensive analysis of the impact of automated cooling system control and sensor feedback on the efficiency of thermoelectric energy recovery.

Thus, this research focuses on a thermoelectric energy recovery system designed for industrial heat exchanger tubes, with a counter-flow cooling system and a process control system for temperature and flow control.

1.2 STATEMENT OF THE PROBLEM

Industrial systems also generate a large amount of unused thermal energy in the form of heat exchanger tubes, boilers, and pipes. Unused thermal energy reduces system efficiency and leads to higher costs and increased greenhouse gas emissions. Although Thermoelectric Generators (TEGs) have the potential to convert heat directly into electricity, there are still significant challenges, including low efficiency, temperature differences between the two bodies, and the lack of automated control systems.

Moreover, most previous studies have focused on theoretical modelling or the isolated performance of TEG, without considering the controlled heat-exchange system. This creates a research gap in developing and experimentally validating a TEG-based waste heat recovery system equipped with automated thermal regulation.

1.3 Aim and Objective of the Research

1.3.1 AIM

The aim of this project is to utilise the amount of energy recovery from potential industrial processing (Counter Heat Exchanger Process) using thermoelectric generator devices (TEG) and process control system.

1.3.2 OBJECTIVES

The following are the objectives of this project:

i. To design a counter-flow heat exchanger system capable of recovering waste heat from industrial processes.

ii. To integrate thermoelectric generator (TEG) devices into the heat exchanger system for converting recovered thermal energy into electrical energy.

iii. To develop a process control system for monitoring and regulating the operating conditions of the heat recovery system.

iv. To analyze the overall performance and feasibility of the integrated heat recovery, thermoelectric generation, and process control system for industrial energy recovery applications.

1.4 SCOPE OF STUDY

This study focuses on the investigating the recovery of waste heat from an industrial process using thermoelectric generator. The research includes the design, installation, testing of a TEG system and the implementation of a process control system to monitor temperature and electrical output. The study evaluates the performance and efficiency of the system under controlled condition.

1.5 SIGNIFICANCE OF WORK

The relevance of this project lies in its ability to provide a solution to one of the biggest problems in industrial processes: the loss of waste heat in heat exchanger tubes. In most industrial setups, significant heat is lost through pipelines, boilers, and condensers, affecting the overall process performance. The TEG system helps to reduce this disadvantageous energy waste by converting it into electrical power.

CHAPTER TWO

LITERATURE REVIEW

2.1 Overview of the Waste Heat Recovery

Industrial processes in the power, chemical, and oil and gas industries generate sufficient amounts of waste heat. It accounts for approximately 20% to 50% of the total energy input in industrial processes that is wasted due to inefficient heat transfer and energy conversion (Snyder & Toberer, 2008). Waste heat has the potential to be a sustainable source of electrical power.

The conventional method of waste heat recovery, including Organic Rankine Cycles, heat exchangers and steam regeneration, has been employed extensively. Nevertheless, these conventional systems tend to be complex, expensive to maintain, and less efficient in varying thermal environments (Bell, 2008).

Thermoelectric generator (TEG) technology offers a promising alternative by directly converting thermal gradients into electricity via the Seebeck effect, without moving parts. This makes TEMs reliable, environmentally friendly, and suitable for both large-scale and localised waste energy recovery (WHR). Moreover, the incorporation of process control technologies such as programmable logic controller (PLC), supervisory control and data acquisition (SCADA), etc.

In a comparative study conducted by Kayfeci (2020), pipelines made of steel, copper, aluminium, and plastic materials were analyzed using numerical simulation and experimental results, with a focus on heat loss. In contrast to conventional fluid transport pipelines, where heat loss is considered undesirable, heat exchangers employ materials with high thermal conductivity (copper or aluminium) and maximize surface area to facilitate efficient heat transfer between working fluids and thermoelectric generator modules (TEMs). By employing this design approach, the objective of recovering waste heat energy and converting it to electrical power can be achieved. Material selection and surface design pipeline and heat exchangers, therefore, play a pivotal role in waste heat recovery (WHR) and thermoelectric power generation

Table 2.1 below shows the thermal conductivity properties of the solid material that can be used for the construction of the pipeline and heat exchanger. The properties will aid in the selection of a material that has high heat conduction properties for use in counter-flow heat exchanger tube. This is expected to improve the efficiency of heat transfer and the output performance of the TEM devices

Table 2.1: Heat Exchanger of the Material and Their Thermal Conductivity

Pipeline / Heat Exchange of the Material	Thermal Conductivity (W/mK)
Aluminum	237
Copper	401
Carbon Steel	50
Stainless Steel	16

The Table 2.2 shows the value of convective heat transfer coefficient of the working fluid flow in the pipeline material and this information will help in choosing various working fluids based on convective heat transfer coefficient of the hot and cold fluid in the design of the model.

Table 2.2: Working Fluid and Their convective heat transfer coefficient

Fluid in the Pipe	Convective Heat Transfer Coefficient (W/m^2)
Water	0.6
Steam	0.026
Oil	0.14

Petrol	0.1
Kerosene	0.12

In steam power plants, carbon steel is commonly used for pipelines because it combines strength, durability, and cost-effectiveness with good resistance to corrosion and erosion, which is essential for high-pressure, high-temperature steam systems (Smith & Johnson, 2020). In contrast, aluminium is often preferred for heat exchanger applications due to its high thermal conductivity, lower cost, and widespread availability.

2.1.1 Heat Loss from a Pipeline from which Steam is Generated from Boiler

The pipeline plays an important role in the transportation of energy resources from one component to another component, such as oil, gas, and steam, over a long distance or short distance, depending on the purpose. These pipelines result in two major energy losses, which are the frictional loss and the pressure or head loss. The transport of heavy oil can result in other forms of energy loss, such as heat loss through modes of heat transfer, including convection and conduction (Bird, 2007). They applied the principle-based model to determine heat losses in a heavy oil pipe that has been disrupted in its working fluid operation, while the pipe is uninsulated and exposed to harsh winter conditions in their country. Based on the aforementioned heat loss challenges, Bahadori (2015) carried out research to estimate the heat loss generated from the surface containing heavy oil in Canada.

2.1.2 Additional Considerations

There are a number of other factors that can affect the heat loss from a pipeline, including:

i. Insulation: The insulation of a pipeline can significantly reduce heat loss. Insulation is typically made of a material such as fibreglass or foam rubber.
ii. Pipe size: The larger the pipe, the more heat will be lost.

By considering all these factors, it is possible to design and install a pipeline system that minimises heat loss from the boiler and maximises efficiency, as per Bahadori (2015).

2.2 The construction of the Thermoelectric Modules

A thermoelectric module (TEM) typically consists of multiple pairs of P-type and N-type semiconductor elements connected electrically in series and thermally in parallel. Metal electrodes are attached to each side of the semiconductor layers to collect the electrical current generated.

The materials commonly used for TEM construction are chosen to maximise the Seebeck effect while maintaining suitable electrical and thermal properties:

i. P-type semiconductor: Bismuth telluride (Bi_2Te_3) doped with antimony (Sb), typically represented as $Bi_{2-x}Sb_xTe_3$.
ii. N-type semiconductor: Bismuth telluride (Bi_2Te_3) doped with selenium (Se), typically represented as $Bi_2Te_{3-x}Se_x$.

These materials are preferred because they provide high thermoelectric efficiency at moderate temperatures (approximately 200–400 K), exhibit good electrical conductivity, and maintain low thermal conductivity. This combination enhances the Seebeck effect, enabling efficient conversion of heat into electrical power (Snyder & Toberer, 2008).

2.2.1 Fundamentals of Thermoelectric Generation

The Seebeck effect is the primary principle utilized in TEGs. It states that when two dissimilar conductors or semiconductors are joined at two junctions and exposed to different temperatures, an electromotive force (EMF) is generated (Champier, *et.al.,*2017). The formula of the voltage output of TEG is

$$V = n.\alpha \cdot \Delta T \tag{2.5}$$

Where:s

n = number of TEMs

α = Seebeck coefficient

ΔT=temperature difference across the junction

The Peltier effect, on the other hand, refers to the absorption or release of heat at the junctions of two different materials when an electric current flows through them. These three effects collectively form the basis of thermoelectric devices.

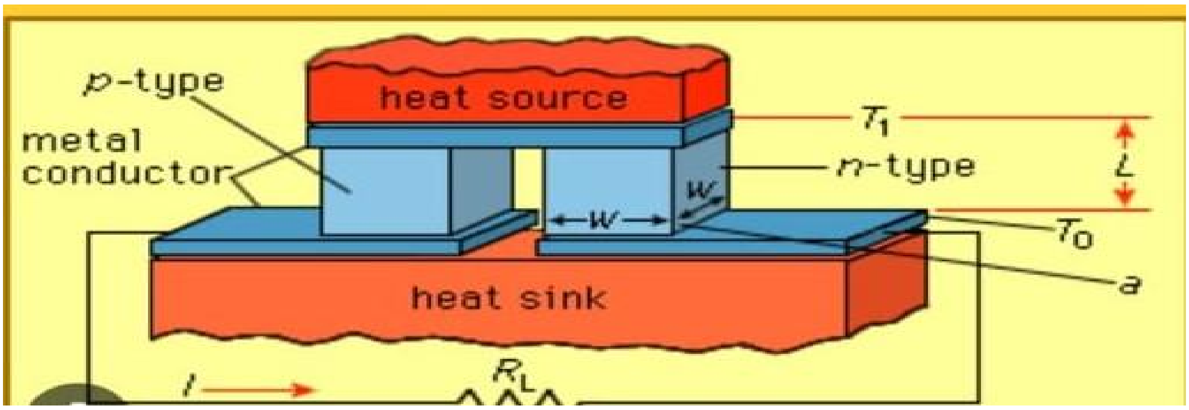

From the above diagram in Figure 2.1, the p-type semiconductor is the positive charge carrier (holes). In contrast, the n-type semi-conductor is the negative charge carrier (electron), I is the current, R_L is the resistor load, L is the height of semiconductor and w is the width of the two semiconductor materials, T_1 and T_0 are the temperature difference on the surface of both heat source and heat sink.

Figure 2.1: Showing the P-type and N-type Semi-Conductor material of TEM

charged carriers) as charge carriers. It is created by doping an intrinsic semiconductor material (e.g., silicon or germanium) with an impurity atom that has one less valence electron than the semiconductor atoms. This creates a deficiency of electrons, leaving behind positively charged holes.

An N-type semiconductor is a semiconductor material with a majority of free electrons as charge carriers. It is created by doping an intrinsic semiconductor material with an impurity atom that has one more valence electron than the semiconductor atoms. This creates an excess of electrons, which become the majority charge carriers.

The TEG does not rely solely on a hot body to produce electricity. As shown in Figure 3.1, it depends on both hot and cold bodies to generate a certain voltage, and it utilizes the temperature difference between the hot and cold sides of the device. This temperature gradient generates voltage through the Seebeck effect, which operates across the depletion layer.

2.2.2 SEEBECK EFFECT ON THERMOELECTRIC GENERATOR

The Seebeck effect is a fundamental thermoelectric phenomenon where a temperature difference across a material generates a voltage. In a thermoelectric generator (TEG), this effect converts heat into electrical energy.

a) **Advantages**:

i. No Moving Parts: Increases reliability and reduces maintenance.

ii. Compact Size: Can be integrated into various systems without significant space requirements.

iii. Environmentally Friendly: Utilises waste heat, contributing to energy efficiency.

b) Challenges:

i. Efficiency: Current thermoelectric materials have relatively low conversion efficiencies (typically between 5-10%).

ii. Material Cost: Some effective thermoelectric materials can be expensive to produce.

iii. Thermoelectric generator (TEG) and the Peltier effect are closely related concepts centred on thermoelectricity, but they serve different functions.

2.2.3 The Connection of the TEMS

In a series arrangement of thermoelectric generator modules (TEMs), the individual TEMs are connected with the positive terminal of one TEM connected to the negative terminal of the next.

This arrangement has several advantages over a parallel arrangement such as follows:

i. Higher voltage: The output voltage of a series arrangement is the sum of the output voltages of the individual TEMs. This means that a series arrangement can generate a higher voltage than a parallel arrangement, which is important for many applications.

ii. Lower internal resistance: The internal resistance of a series arrangement is the sum of the internal resistances of the individual TEMs. This means that a series arrangement has a lower internal resistance than a parallel arrangement, which reduces power losses.

iii. Higher power output: The power output of a TEG is proportional to the product of the voltage and current. Since a series arrangement has a higher voltage and lower internal resistance, it produces more power than a parallel arrangement.

2.3 POTENTIAL APPLICATIONS

TEG Applications in Waste Heat Recovery (WHR)

The application of TEG technology in industrial environments has attracted attention for its compact design, scalability, and ability to generate clean electricity from waste heat**.**

2.3.1 Automotive and Aerospace Sectors

The automotive sector led the integration of TEGs into the exhaust systems of internal combustion engines to enhance fuel efficiency (Muhammad Irfan Khan *et al*., 2024). General Motors and BMW have shown the feasibility of TEG-based systems that produce a maximum of 500 W of electrical power from exhaust gases, thereby reducing the load on the alternator (Nolas *et.al.,* 2001). Likewise, in the aerospace sector, TEGs produce power in satellites by harnessing the waste heat from radioactive processes or propulsion systems to produce electricity (Snyder and Toberer, 2008).

2.3.2 Industrial Heat Exchangers and Pipelines

Recent research has focused on mounting TEG modules on heat exchange tubes in boilers, condensers, and chemical reactors (Montecucco and Siviter, 2016). In such setups, TEGs

INDUSTRY	HEAT SOURCE	TEMP RANGE VALUE	POWER OUTPUT FROM THE TEG	SUITABLE APPLICATION
Automotive	**Exhaust gas**	**300–600°C**	**300–500 W**	**Improves fuel economy**
Industrial pipelines	**Process fluids**	**150–300°C**	**50–200 W**	**Suitable for distributed sensors**
Power plants	**Boiler surfaces**	**200–400°C**	**500–1000 W**	**Requires large module arrays**

utilize the high surface temperature of heat exchangers and pipelines to recover energy without disrupting the process flow. Studies have shown that installing TEG arrays along pipelines can generate supplementary power for sensors, actuators, and monitoring systems (LeBlanc, 2014).

Table 2.3: **A Table of Comparison of TEG implementations in Different Industries**

The table 2.3 show the previous result of the installation of TEG and how the temperature difference was capable to generate certain amount of power for various application.

2.3.3 Previous Research on TEG Applications in Waste Heat Recovery

Some research has been conducted to investigate the feasibility of TEG systems in industrial waste heat recovery. For instance, Crane and Jackson (2004) investigated the use of TEG in heat exchangers and concluded that with appropriate design and integration, a temperature difference can be utilized to generate useful power. In another research, (Dai et al. 2015) designed a heat pipe-TES system that showed enhanced performance compared to the conventional system.

2.4 Process Control with PLC Integration

Programmable Logic Controllers (PLCs) and sensors are important components for monitoring system parameters such as temperature differences, voltage, and current, and for implementing control strategies. A PLC-based system can:

i. Control the power electronics stage (e.g., adjusting duty cycles in DC-DC converters)
ii. Provide fault detection and alarms for overheating or underperformance

This level of automation improves system reliability and efficiency, especially in industrial environments where continuous monitoring is required.

2.5 RESEARCH GAP

2.5.1 Research Gap and Motivation

Research Gap and Motivation

The results obtained from the literature survey have verified that a substantial amount of thermal energy in industrial processes is wasted in the form of waste heat, especially from heat exchanger tubes, pipes, and other heat transfer surfaces. Although the concept of thermoelectric generator (TEG) technology has been well accepted as a promising solution for the direct conversion of waste heat into electrical energy, its practical application on a large scale is still hindered by low conversion efficiency and unstable output performance due to fluctuating thermal inputs. Most of the existing literature has been devoted to the improvement of thermoelectric material properties or the design of heat exchangers, but very little attention has been paid to the real-time monitoring and control of TEG system performance.

Moreover, the output voltage of TEG modules is generally low and highly dependent on the temperature gradient variations, which makes the electrical output unsuitable for direct use in domestic or industrial applications without any conditioning. Nevertheless, there is still a lack of adequate literature on the use of process control systems, voltage regulation methods, and power amplification circuits necessary for stabilizing and upgrading the output power of TEG systems.

CHAPTER THREE

MATERIALS AND METHODS

3.1 Description of Concept

The arrangement of five thermoelectric generator modules in series is shown in Figure 3.1. The arrangement, simulated using Proteus software, positions the hot-side heat exchanger in direct contact with a heat source and the cold-side heat exchanger in direct contact with a heat sink. Since the five thermoelectric generator modules are in series, the total voltage developed is the sum of the individual voltages. The total voltage developed is then measured using a multimeter.

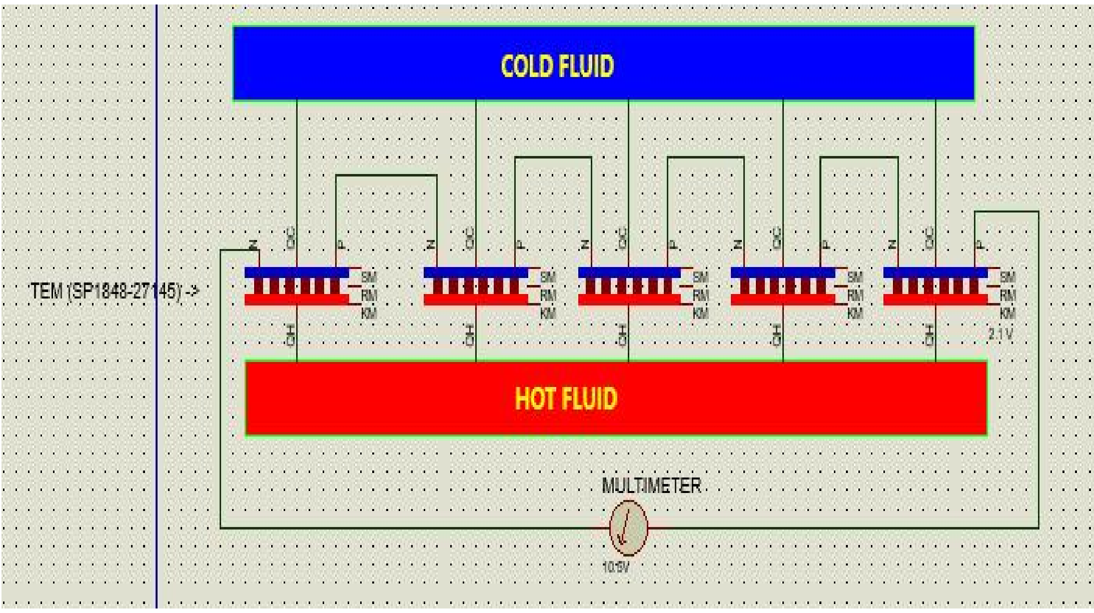

Figure 3.1: A Schematic illustration of the TEM using Proteus

In this chapter, the various materials and methods used for this project are discussed, including the reasoning behind the selection of each material and the methodology applied. The aim is to determine whether the selected approach is feasible and to use mathematical methods to calculate the heat in the system on the both surfaces of the thermoelectric modules (TEM) in order to produce voltage and current in the system process.

The hot-side temperature can be obtained from the heat lost to the environment, while the cold-side temperature requires a heat sink and the application of a simple cooling system concept to create and maintain the necessary temperature difference. Calculation software will be employed to analyse and optimise the process and method. A small-scale prototype will be designed and tested to demonstrate the concept and evaluate its suitability for real-world applications.

3.2 Material and Component Selection

Before presenting the various materials considered for investigating energy recovery from heat exchanger pipelines or tube surface heat losses using TEG devices and a process control system, a decision matrix was developed. This matrix was based on the specifications and performance criteria of the different components involved.

The components are

1. Steam cycle (Thermal Cycle components)
    a) Boiler body
    b) Condenser

2. Electronics components
    a) Veo board, breadboard, etc
    b) Thermoelectric devices (Peltier modules- seebeck effect)
    c) Arudino (Uno, Micro, Mega, Nano etc)
    d) Wire (such as Banana wire and jumper wire)
    e) LCD (liquid crystal display: 16 x 2 LCD (Hitachi HD44780), 128x64 LCD (SHARP LS12864-1), TFT LCD (Thin-Film Transistor-ILI9341), 20 x 2 Monochrome LCD(HMCO2OL))
    f) Voltage senor (10M ohm voltage divider, Zener diode voltage or IN4733A, Voltage reference IC voltage sensor or REF1112)
    g) Current sensor (ACS712 30A, INA250, SCT-013)

3. Mechanical Components
    a) Heat sink and water cooling heat exchanger tube (Aluminium, copper, stainless steel.)
    b) Tubes
    c) Thermal paste
    d) Pump
4. Reservoir or cooling tower
    a) Condenser
    b) Block of ice

c) Mini water pump device

d) Cooling fan

e) Cool water tank (Reservoir)

5. Control system and simulation tool

a) S-scope soft for displaying the voltage in the oscilloscope

b) Power amplifier

c) Measuring device such as Multimeter, Vernier Caliper, Thermocouple etc.

d) Proteus, Matlab, Solidwork and Tinkercad for simulation process.

3.2.1 Cycle description components for thermal power (thermal cycle components)

1. Steam cycle

In this project, the steam leaving the boiler passes through the inner tube of the aluminium water-cooled heat sink serving as the heat source for the Seebeck process in the TEG before entering the heat sink. Heat is conducted from the tube to the surface of the aluminium heat sink, resulting in a temperature drop. This heat is then transferred to the upper side of the TEG, forming its hot side. A layer of thermal paste is applied between the tube and the TEG to provide a conductive interface and ensure efficient heat transfer.

a) Boiler body

The boiler needs a pressure vessel that can resist high temperatures and internal pressures, just like a gas cylinder. The choice of material for the boiler shell needs to take into account critical properties such as wall thickness, which is necessary for the design pressure, mechanical strength, and resistance to high temperatures.

b) Tubes

For transporting the steam, heat-resistant tubing, like silicon or copper, was chosen based on its resistance to higher temperatures. The heat source for the boiler was designed using a burner system. The heat input could be provided either by an electric heating element or by using combustible fuels like alcohol or gas hydrocarbons (methane, ethane, propane).

c) Housing

A protective housing was designed to integrate and secure all boiler components. This enclosure ensures safe operation, thermal insulation, and protection of the system from external disturbances.

3.2.2 Electronics components

a) Vero Board and Breadboard

Vero boards, also known as stripboards, are perforated board with parallel copper strips that serve as electrical connections and it is used for constructing permanent electronic circuits. They require soldering to create electrical connections (permanent circuit assembly), making them suitable for long-term projects and industrial applications. These boards are commonly used for prototypes and small-scale production.

Breadboards, on the other hand, are solderless prototyping boards that allow easy circuit construction and testing. They contain interconnected rows and columns for component placement and wiring without permanent connections. Breadboards are reusable and widely used in educational, research, and industrial environments for rapid prototyping. It consists of rows and columns of interconnected holes for inserting components and jumper wires.

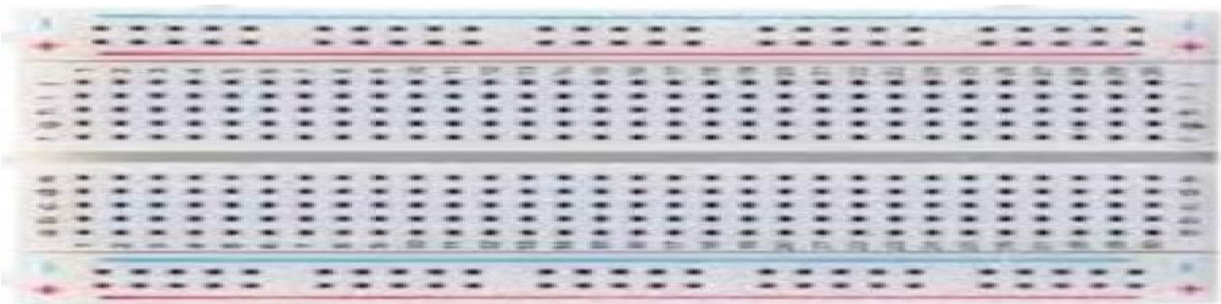

Figure 3.2: Breadboard

Table 3.1 Thermoelectric Devices

Components	Description	Features

I. SP1848-27145	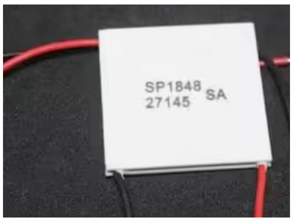 Figure 3.3: **SP1848-27145**	i. **Dimensions:** 40 mm × 40 mm × 3.6 mm ii. **Operating Temperature:** 30°C – 150°C iii. **Voltage Output:** 4–6 V at ΔT of 100°C **Power Output:** 4 W (approx.)
II. TEC1-12706	 Figure 3.4: TEC1-12706	i. **Voltage:** 12 V ii. **Current:** 6A iii. **Power:** 72 W
III. TEC1-12710	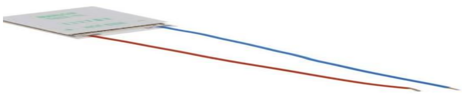 Figure 3.5: TEC1-12710	i. **Voltage:** 12 V ii. **Current:** 10 A iii. **Power:** 120 W
IV. **TEG1-12611-6.0**	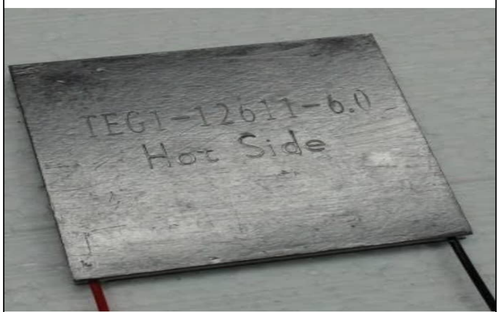 Figure 3.6: TEG1-12611-6.0	i. **Dimensions:** 50 mm × 50 mm × 4 mm ii. **Voltage Output:** 6 V at ΔT of 100°C iii. **Current:** 1.2 A **Power Output:** ~7 W.
V. GM-TEC1-12715		i. **Voltage:** 12–15 V ii. **Current:** 15 A iii. **Power:** 180 W (as a cooler

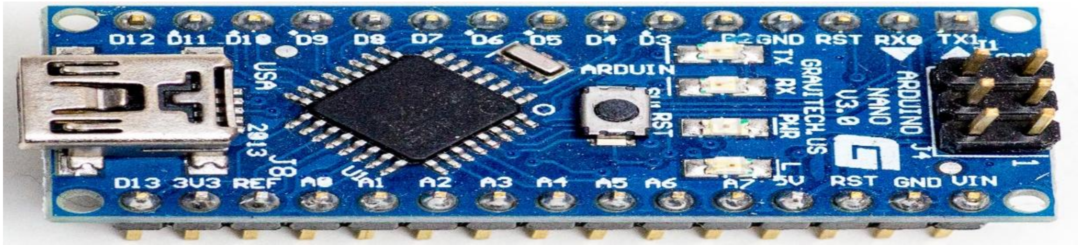

Arduino Boards (Uno, Due, Micro, Mega, Nano)

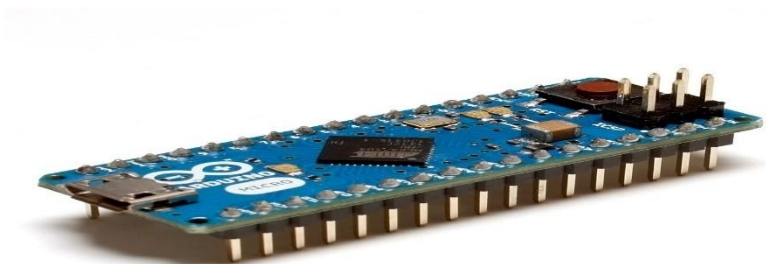

Figure 3.8: Arduino Mega

Figure 3.9: Arduino Nano

b)

Figure 3.10: Arduino Micro

Banana wires are flexible wires with banana plugs at their ends, used for connecting laboratory instruments such as power supplies and Multimeters. They offer quick and secure connections during testing and measurements. Jumper wires are thin insulated wires used for connecting components on a breadboard or header pins.

Figure 3.11: Banana wire

Figure 3.12: jumper wire

c) LCD (Liquid Crystal Display)

LCDs are used to display sensor readings, such as voltage, current, and temperature. Common types include:

i. 16 x 2 LCD (Hitachi HD44780): Displays 16 characters on two rows, commonly used in Arduino projects
ii. 128 x 64 LCD (Sharp LS12864-1): Graphic display for complex data visualisation.
iii. TFT LCD (ILI9341): High-resolution colour display used in advanced embedded systems.

iv. 20 x 2 Monochrome LCD (HMC020L): Displays 20 characters per line in two rows, suitable for data logging.

d) Voltage Sensors

Voltage sensors are used to measure and monitor the electrical voltage generated by TEG modules.

i. 10MΩ Voltage Divider: Simple and low-cost solution for scaling down high voltage to safe levels for microcontrollers.

Figure 3.13: 10MΩ Voltage Divider

ii. Zener Diode Voltage Sensor (IN4733A): Maintains reference voltage using reverse breakdown characteristics.

iii. Voltage Reference IC (REF1112): Provides a high-precision reference for ADC calibration and stable measurements.

e) Current Sensors

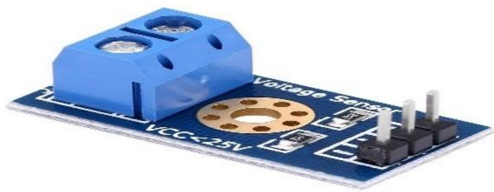

Current sensors measure current in circuits for monitoring power output and detecting overcurrent conditions.

I. ACS712 (30A): Hall-effect sensor capable of measuring both AC and DC currents up to 30A.

Specification

Figure 3.14: ACS712 (30A)

i. Supply Voltage: 4.5V

ii. Current (I_{SENSE}) =30A

iii. G- Gain: ACS712 Sensitivity: 66mV/A

II. INA250: Features integrated current shunt and precision amplifier for accurate measurements.

Specification

i. POWER OUTPUT (G- Gain): INA250A1- Q1 200 mV/A

Figure 3.15: INA250

ii. Current (I_{SENSE}) = –10 A to 10 A

III. SCT-013: A non-invasive current transformer for AC current measurement without direct contact with the conductor.

Figure 3.16: SCT-013

3.2.3 Mechanical Components

a) Heat sink and water cooling heat exchanger tube (Aluminium, copper, stainless steel, brazed plate fin heat exchanger.)

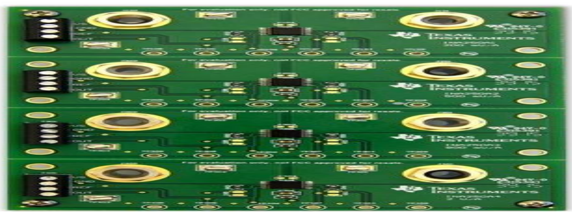

Serves as the primary interface for heat transfer

Aluminum: Lightweight, cost-effective, and excellent thermal conductor. Example of the material is water cooling head efficient heat dissipation sink (aluminum)

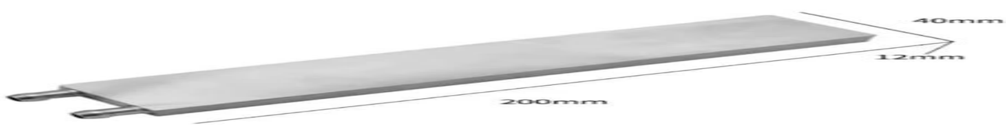

Figure 3.17: Heat sink and water-cooling heat exchanger tube (Aluminum)

b) **Tubes (inlet and outlet):**

Provide a pathway for circulating hot and cold water between the heat exchanger and the reservoir. They ensure continuous flow for steady heat transfer.

c) **Thermal paste (thermal interface material):**

Figure 3.18: (**Thermal paste**)

Enhances thermal conductivity between the TEG modules and the water cooling and heat sink disspation surfaces by eliminating air gaps, thereby improving energy conversion efficiency.

d) Pump

Maintains and regulates the flow rate of water through the system. This ensures controlled heat transfer and helps sustain the desired temperature gradient for TEG operation. It transfer liquid from one point to another.

i. Centrifugal Pump

Centrifugal pumps convert rotational kinetic energy to fluid flow using an impeller. They are

ii. DC Submersible Mini Water Pump

.

Figure 3.19: DC Submersible Mini Motor Pump

iii. Mini Water Pump ZYW680 (DC 24 V, 5.5 m Lift, Brushless Motor)

.

Figure 3.20: (Mini Water Pump ZYW680 (DC 24 V, 5.5 m Lift, Brushless Motor))

3.2.4 Reservoir or cooling tower

a) Condenser

A condenser is a heat exchanger designed to condense steam or hot vapor back into liquid by removing latent heat.

b) Block of ice

A block of ice is sometimes used in experimental setups as a low-cost, simple cold sink. It maintains a very low temperature for the TEG's cold side, maximizing ΔT and boosting voltage output. However, it is only practical for short-term or laboratory-scale applications.

c) Cooling fan

A cooling fan assists heat dissipation on the cold side of the TEG by forcing air over a heat sink or radiator. This improves convective heat transfer and lowers the cold-side temperature. Fans are cost-effective and simple to control via PWM (Pulse Width Modulation). It also supports low temperatures on the water cooling side of the heat exchanger.

d) Mini Water Pump Device

A mini water pump (DC submersible or brushless type) circulates the coolant through the heat exchanger tubes, radiator, or reservoir. It ensures steady heat transfer by maintaining constant flow, which stabilizes ΔT and improves TEG efficiency. Low-noise, low-power pumps are preferred for compact TEG systems.

e) Cool water tank (Reservoir)

A cool water tank acts as a thermal buffer, storing cold water to absorb heat from the TEG's hot side. By ensuring a constant supply of relatively cool water, it maintains ΔT and avoids rapid temperature rise in the coolant loop, which would reduce TEG performance.

3.2.5 Control system and simulation tool

A robust control system is essential for optimising the performance of a thermoelectric generator (TEG)-based energy recovery system. This section explains the major control elements, measuring devices, and software tools used for process monitoring, control, and system simulation, all of which are key to maximizing the power output and efficiency of the TEG system. The process control system regulates the flow rate of hot and cold fluids to maintain a steady temperature gradient (ΔT) across the TEG modules. A PLC or Arduino-based controller can monitor input signals from temperature sensors, thermocouples, and voltage/current sensors. Feedback loops automatically adjust pump speed, fan operation, or valve position to ensure optimal heat transfer and power generation. Control logic ensures that the output voltage remains within the desired operating range, thus improving system stability.

a) S-Scope Software (Oscilloscope Display)

S-Scope software is used to display voltage and current waveforms from the TEG system in real-time. This allows researchers to visualize transient behaviors such as voltage fluctuations due to changes in heat input or flow rate, enabling fine-tuning of PID controllers for maximum power output.

b) Power Amplifier

A power amplifier boosts the low-voltage DC output of the TEG modules to a usable level for driving loads or charging batteries. It enables regulation of output voltage and allows efficiency testing under different electrical loading conditions.

c) Measuring Devices

Accurate measurement is critical for validating experimental results:

3.3. Design Matrix for the Selection of the Material

A decision matrix is a systematic tool for evaluating and comparing multiple alternatives against a set of predefined criteria. In this project, it is used to guide the selection of mechanical, electrical, and control components that maximise efficiency in recovering waste heat using thermoelectric generator (TEG) devices.

Purpose of Decision Matrix

i. To provide an objective framework for selecting the most suitable components.
ii. To balance performance, cost, durability, efficiency, and ease of integration in the system.
iii. To minimize bias in choosing components by applying a quantitative scoring system

Compare alternatives objectively we use the same scoring criteria for every category (scale 1–5; 5 = best). Weights reflect the relative importance:

i. Cost — **0.20**
ii. Efficiency / Accuracy — **0.30**
iii. Durability / Reliability — **0.15**
iv. Ease of integration — **0.15**
v. Availability — **0.10**
vi. Maintainability — **0.10**

Weighted score per option = $\sum(i \times j)$. Scores are justified briefly below each table.

where

i = score

j = weight

$\sum$ = sum

In summary, after considering the decision matrix for each of the components. The best material selected for the design for the investigation of the energy recovery from the heat exchange tube by using thermoelectric generator and process control device are shown in the table below. The cell in the table that indicate red on the background in the cell in the table, implies that material is consider for the detail design due to two factors, one the weighted total and the availability of the materials

Table 3.2: Weighted Score of The Decision Matrix for All The Components

Various components unit	Option A	Option B	Option C	Option D
Mechanical components				

Heat exchanger tubes	Aluminium	Copper	Stainless steel	Brazed plate-fin
Pump	Centrifugal	Rotary	Micro DC (3–6V)	ZYW680 (24V brushless)
cooling device	Fan (air)	Cool water tank (reservoir)	Cooling tower	Block of ice
Electronic components				
voltage sensor	Voltage divider (10MΩ)	Zener (IN4733A)	REF1112 (voltage ref)	
current sensor	ACS712 (30A)	INA250	SCT-013	
LCD	TFT ILI9341	16×2 HD44780	128×64 LS12864-1	20×2 HMC020L
Control hardware component	PLC	Arduino Uno/Nano	Arduino Du	Process control
Power conditioning	Simple boost converter	MPPT DC-DC (dedicated)	Inverter + Battery	
TEG	SP1848-27145	TEC1-12706	Marlow TG series	Hi-Z HPM series

The decision matrix, outcome from Table 3.1 to select the material that will be used in building the concept from the block diagram for the investigation of the project.

i. Heat exchanger (Aluminium)
ii. Pump (Mini DC motor pump)
iii. Cooling device (Cool water tank (reservoir) and fan for further cooling of the cool water side for better efficiency)
iv. Voltage sensor (Voltage divider (10MΩ))
v. Current sensor (ACS712 (30A))
vi. LCD (16×2 HD44780 or 12c)
vii. TEG (SP1848-27145)
viii. Power conditioning (Inverter + Battery)

ix. Control hardware component (Arduino Uno/Nano for sensor and process control for the monitor and amplify the voltage from the TEG)

3.3.1 Detailed Design

The first concept was to design boiler of a small prototype of steam cycle and cooling cycle. The both cycle will be connected together to heat exchanger. That means the steam power cycle system and the refrigerator cycle will have connected by heat exchanger in between them. The heat exchanger is the substance that permit the hot fluid from the steam cycle and cold fluid from the cooling cycle to flow through it by the means of indirect contact between them. the thermoelectric generator measures the temperature difference between the two fluids and convert it electricity by generating voltage.

The design of the second concept only required the refrigerator cycle system or cooling tower cycle that supply cold fluid, that will flow through the sink. This design of the second concept will be tested from the heat of the exhaust pipe of the generator and comparing the temperature of the cold fluid to that of the temperature for exhaust pipe of generator to generate the amount of voltage the will used to power some electronic components.

The block diagram of the concept is show in Figure 3.21 and material considered from the decision matrix

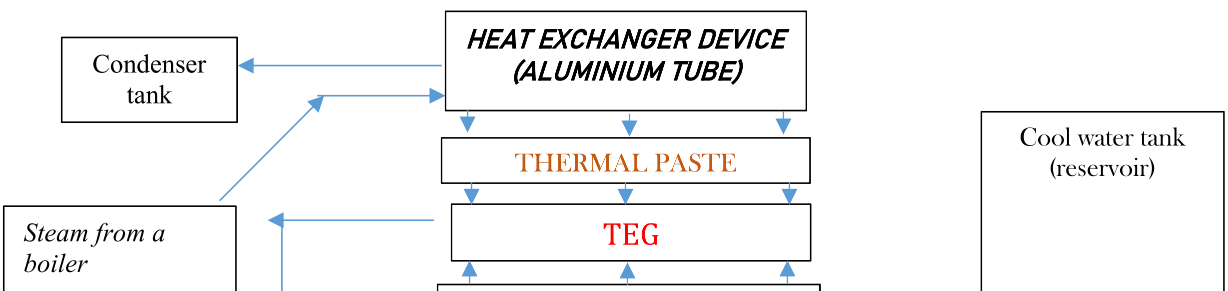

Figure 3.21: BLOCK DIAGRAM FOR THE CONCEPT

3.3.2 CAD Model Overview

The overall thermoelectric generation unit has been modelled using SolidWorks to give a detailed representation of the system's layout. The system design combines the boiler, hot and cold heat exchangers, thermoelectric modules(TEMs), and the cooling unit into one assembly, focusing on both system organisation and component alignment.

The model illustrated in Figure 3.22 can show the alignment of components and the flow of heat within the core system structure. A lot of focus has been placed on the geometry to ensure that the system has a realistic representation. The CAD system model is a precursor to further analysis and fabrication design, giving a clear visual representation of the system layout. Figure 3.23 illustrate the measurement and dimension of the rig design for experimental work in 2 dimensional representation

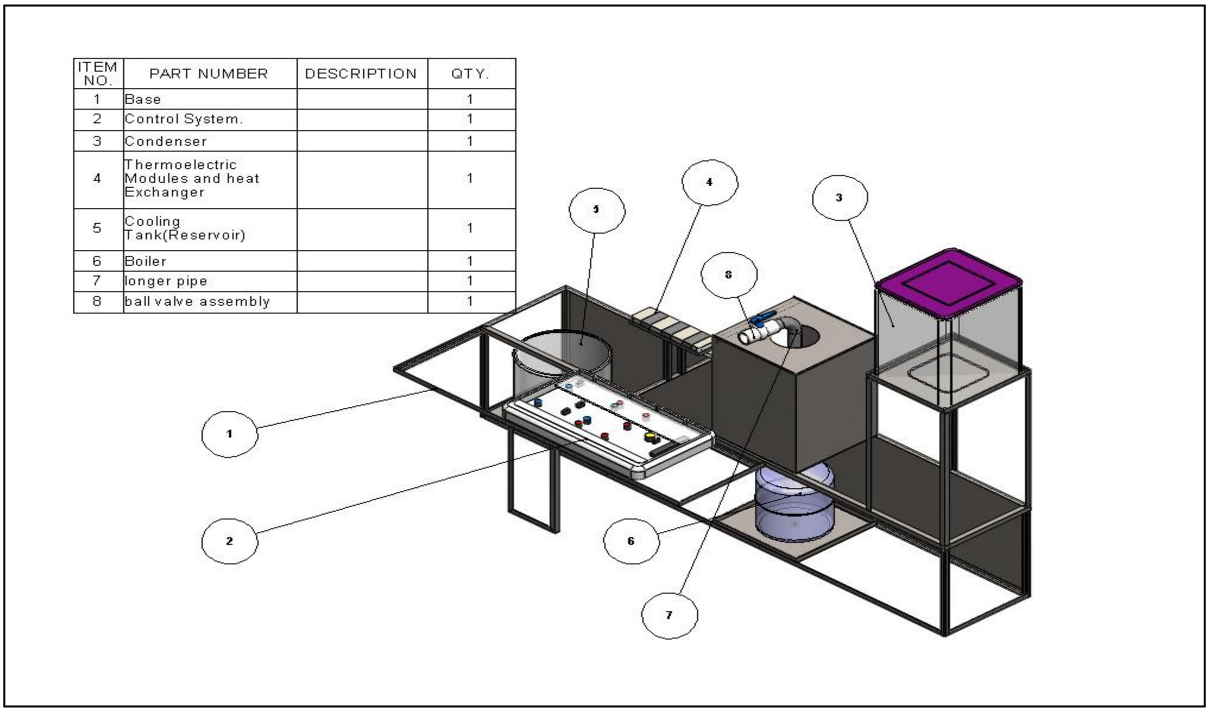

ITEM NO.	PART NUMBER	DESCRIPTION	QTY.
1	Base		1
2	Control System.		1
3	Condenser		1
4	Thermoelectric Modules and heat Exchanger		1
5	Cooling Tank(Reservoir)		1
6	Boiler		1
7	longer pipe		1
8	ball valve assembly		1

Figure 3.22: 3D Drawing with bill of Material in solidwork presentation

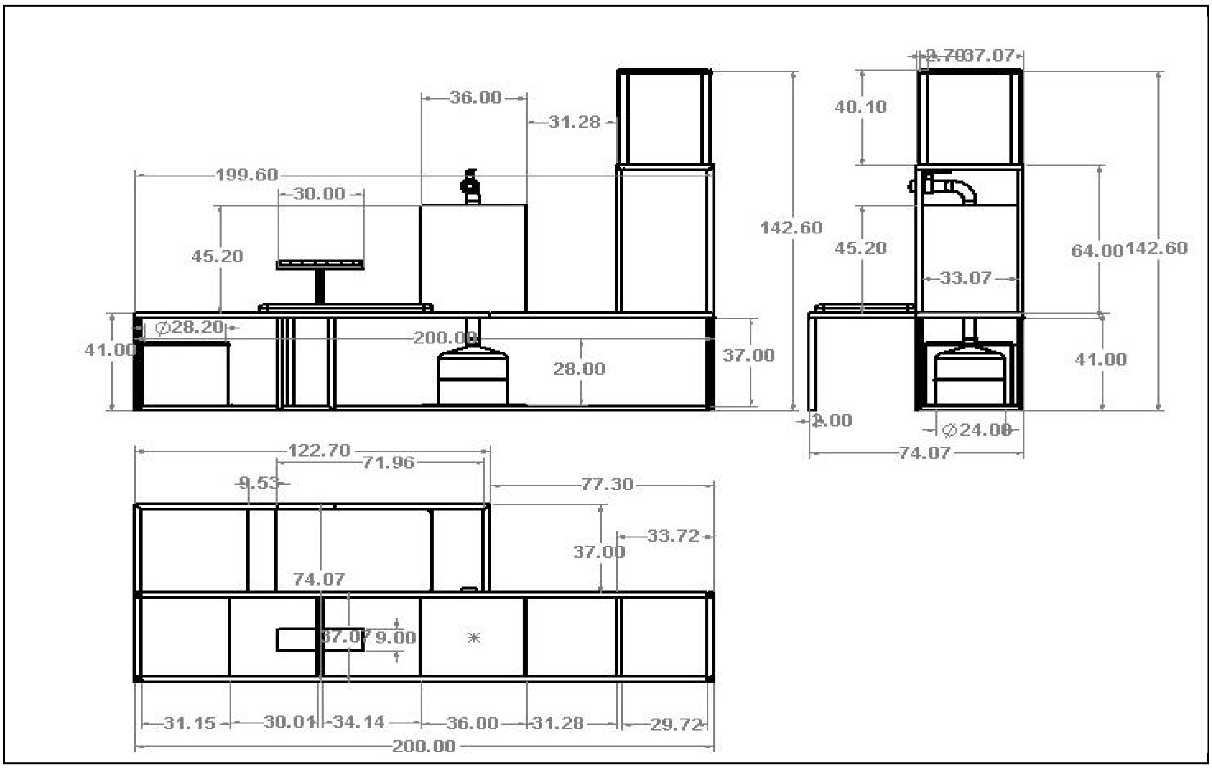

Figure 3.23: 2D Representation with Measurements

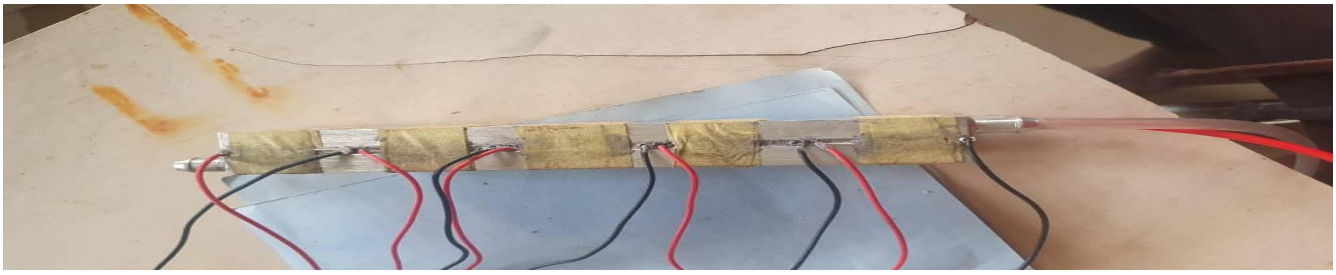

Figure 3.24: The image of the heat exchanger devices with terminal wire

3.3.3 Method and formula used based real and simulation concept

To understand the method, flow process is show Figure 3.3.4 for the heat exchange to transfer energy to the TEG to generate the Electrical energy

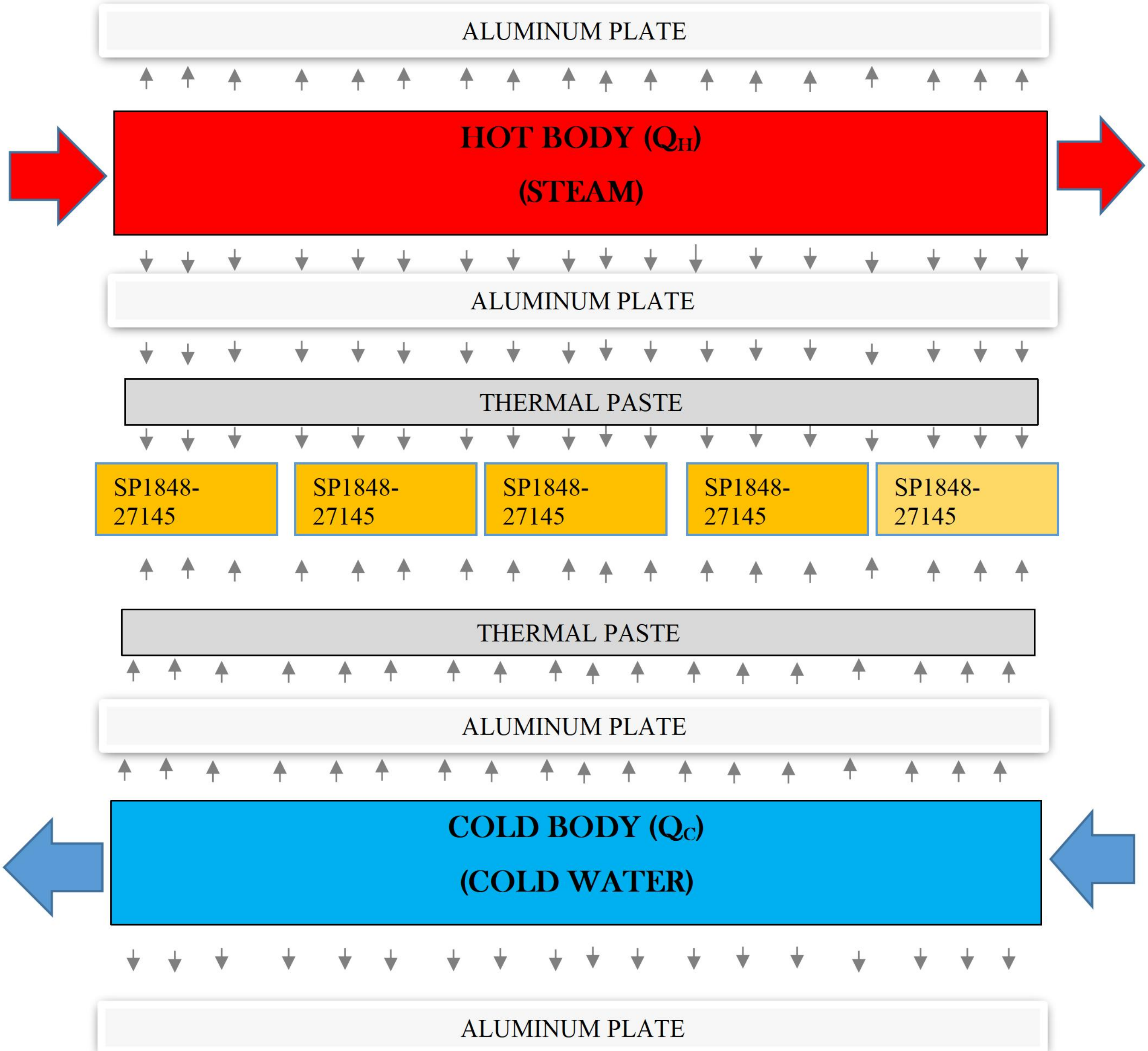

FIGURE 3.25: The section of the TEG and direction of the flow for the two bodies (hot and cold)

In Figure3.25, the heat flows downward to the thermal paste to the TEG by means of conduction. The red block, right arrow, and left arrow show the flow direction indication of the steam flow in and out of the tube of the heat exchanger device to the condenser tank, while the blue block, right arrow, and left arrow indicate as similar process but for the cold.

3.4 TEG Model Development

3.4.1 Assumption

1. Assumption for the heat exchanger of the pipe and aluminium plate

The following assumptions (Er. R.k. Rajput, 2015) are

i. The overall heat transfer coefficient U is constant.
ii. The flow conditions are steady.
iii. The specific heats and mass flow rates of both fluids are constant.
iv. The changes in potential and kinetic energies are negligible.

2. Assumption for the TEM model

The following assumptions are made for the TEM model

i. Seebeck coefficient, thermal conductivity and electrical resistance of the material change with the average temperature of the two sides of the thermocouple.
ii. The Thomson effect in the TEM can be neglected

3. Assumption for the TEM model

The following assumption are made for TEG model

i. The main heat leakage is the heat flow through the insulation materials. Both radiative and convective heat loss from TEG system to the surroundings are neglected.
ii. The flow rates for both exhaust gas and coolant are assumed to stay constant along the flow direction. Both boiler and the cooling reservoir density variation with temperature change in TEG are sufficiently small to have no practical effect on the predictions.

iii. Heat conduction along the flow rate direction is ignored in each control volume, as heat conduction perpendicular to the flow direction is dominant. Temperature inside each component is uniformly distributed in each volume.

iv. The hot and cold flow of the inlet and outlet of the TEG are assumed to be constant as assumed value due to no sensor.

v. Both pipe head loss from the boiler and the plastic tube head loss from the cooling water reservoir are neglected.

3.4.2 TEG Modelling Equations

a). Heat Transfer Formula in an Aluminium Tube

For the aluminium heat exchanger, the total heat transferred can be determined in Equation 3.1:

$$Q = UA\,\Delta\theta_M \tag{3.1}$$

Where

Q = heat transfer rate (W)

U = overall heat transfer coefficient (W/m²·K)

A = effective heat transfer area (m²)

$\Delta\theta_M$ = log mean temperature difference (LMTD)

b). Logarithmic Mean Temperature Difference LMTD

For counter-flow configuration (cold water flows in and out opposite to the steam to hot water):

$$\Delta\theta_M = \frac{\theta_1 - \theta_2}{\ln\left(\frac{\theta_1}{\theta_2}\right)} \tag{3.2}$$

Where;

θ_1= temperature difference between the hot and cold fluids at the inlet (K)

θ_2= temperature difference between the hot and cold fluids at the outlet (K)

$\theta_n = T_{hn} - T_{cn}$

c). HEAT TRANSFER OF BOTH THE HOT AND COLD FLUIDS

$$Q = \dot{m}c_p\Delta T \tag{3.3}$$

For the hot fluid

$$Q_h =- \dot{m}_h c_p(T_{he} - T_{hi}) \tag{3.4}$$

For the cold fluid

$$Q_c = \dot{m}_c c_p(T_{ce} - T_{ci}) \tag{3.5}$$

Where

Q_h= heat transfer by the hot fluid

$\dot{m}_h$= mass flow rate of the hot fluid

c_p= specific heat capacity of the fluid at a constant pressure(kJ/kgk)

T_{hi}= temperature of the hot fluid at the inlet (k)

T_{he}= temperature of the hot fluid at the exit (k)

Q_c= heat transfer by the cold fluid

$\dot{m}_c$= mass flow rate of the cold fluid

c_p = specific heat capacity of the fluid at a constant pressure(kJ/kgk) (for water = 4.186~4.200 kJ/kgk or 4200 J/kgk

T_{ci}= temperature of the cold fluid at the inlet (k)

T_{ce}= temperature of the cold fluid at the exit (k)

d). Temperature Difference Across Each TEG

Since, the **5 TEGs** equally spaced along the tube, approximate ΔT across each as:

$$\boldsymbol{\Delta T_{teg(n)}} = T_{hn} - T_{cn} \tag{3.6}$$

Where;

T_{hn} and T_{cn} are the hot and cold surface temperatures at the position of the nth of TEG.

If heat loss is small, it assumes nearly constant ΔT across all modules Voltage Generated by

e). Voltage Generated by TEG

TEG Voltage output is related to ΔT by the Seebeck Effect:

$$V = n \cdot S \cdot \boldsymbol{\Delta T_{teg}} \quad (3.7)$$

Where:

n = number of thermocouples inside the TEG (for SP1848-27145, n=127)

S = Seebeck coefficient per thermocouple (≈ 200 μV/K for Bi_2Te_3-based TEGs)

ΔT = temperature difference across the module (K)

For the n and S values, values were obtained from datasheet of **TEM (SP1848-27145)**

$V = 127 \cdot (200\times10^{-6}) \cdot \Delta T$

$$V = 0.0254\, \boldsymbol{\Delta T_{teg}} \quad (3.8)$$

Linking Heat Transfer to Voltage

Linking Heat Transfer to Voltage The overall heat transferred Q affects the temperature difference:

$$Q = UA\,\Delta\theta_M \text{ and } V = 0.0254\, \boldsymbol{\Delta T_{teg}}$$

$$\boldsymbol{\Delta T_{teg(n)}} = \Delta\theta_n = \text{temperature of comparing two bodies}$$

$V \alpha\, \boldsymbol{\Delta T_{teg}} \Leftrightarrow V \alpha\, \Delta\theta_n$

Therefore, this implies

$$V = 0.0254\ \Delta\theta_n \quad (3.9)$$

g). Power and efficiency of TEG system

$$\text{Power of TEG, } P = I\,V \quad (3.10)$$

Efficiency of the system, $\eta = \dfrac{power\, of\, TEG(P)}{heat\, supplied\, in\, the\, system\, (Q)}$ (3.11)

3.4.3 TEG Experiment setup

I. Arrangement of TEM

Since the arrangement of the TEMs is connected in series, the current is constant while the voltage varies.

So the total voltage supplied in the system (V_T)= V_1+ V_2+ V_3+V_4+V_5

Same is applicable to heat supplied in the system, (Q_T)= Q_1= Q_2= Q_3=Q_4=Q_5

The empirical model is often a regression equation.

II. Common model used for TEG power:

The regression gives you coefficients:

Load resistance R_L

Internal resistance Ri

$$P=a_0+a_1(\Delta T)+ a_2\,(\Delta T)^2+a_3R_L+a_4(\Delta T)(R_L)$$

III. Model Validation

To validate the empirical model, predicted efficiency values were calculated using the developed equation and compared with experimental efficiency values. The percentage error was calculated using:

%Error = [(η_exp − η_pred) / η_exp] × 100

Where:
η_exp = experimental efficiency
η_pred = predicted efficiency from empirical model

The model's accuracy was evaluated using the coefficient of determination (R^2).

Empirical Model for Power Output

Similarly, an empirical model was developed for the electrical power output as a function of temperature difference across the TEG module. The polynomial model is expressed as:

$P = b_0 + b_1(\Delta T) + b_2(\Delta T)^2$

Where b_0, b_1, and b_2 are regression constants obtained experimentally.

IV. Scaling Empirical Model Used

The experimental measurements obtained for five thermoelectric modules (5 TEMs) were used as the baseline for empirical prediction of performance for larger TEM arrays. Assuming identical operating conditions, uniform temperature difference across each module, and negligible wiring losses, the output voltage and power were assumed to scale linearly with the number of TEM modules connected in series.

The scaling empirical equations used are:

$V_N = (N/5) \times V\_5$

$P_N = (N/5) \times P\_5$

Where:
V_N = predicted voltage for N TEM modules (V)
P_N = predicted power for N TEM modules (W)
V_5 = measured voltage for 5 TEM modules (V)
P_5 = measured power for 5 TEM modules (W)
N = number of TEM module

A simple illustration of matlab

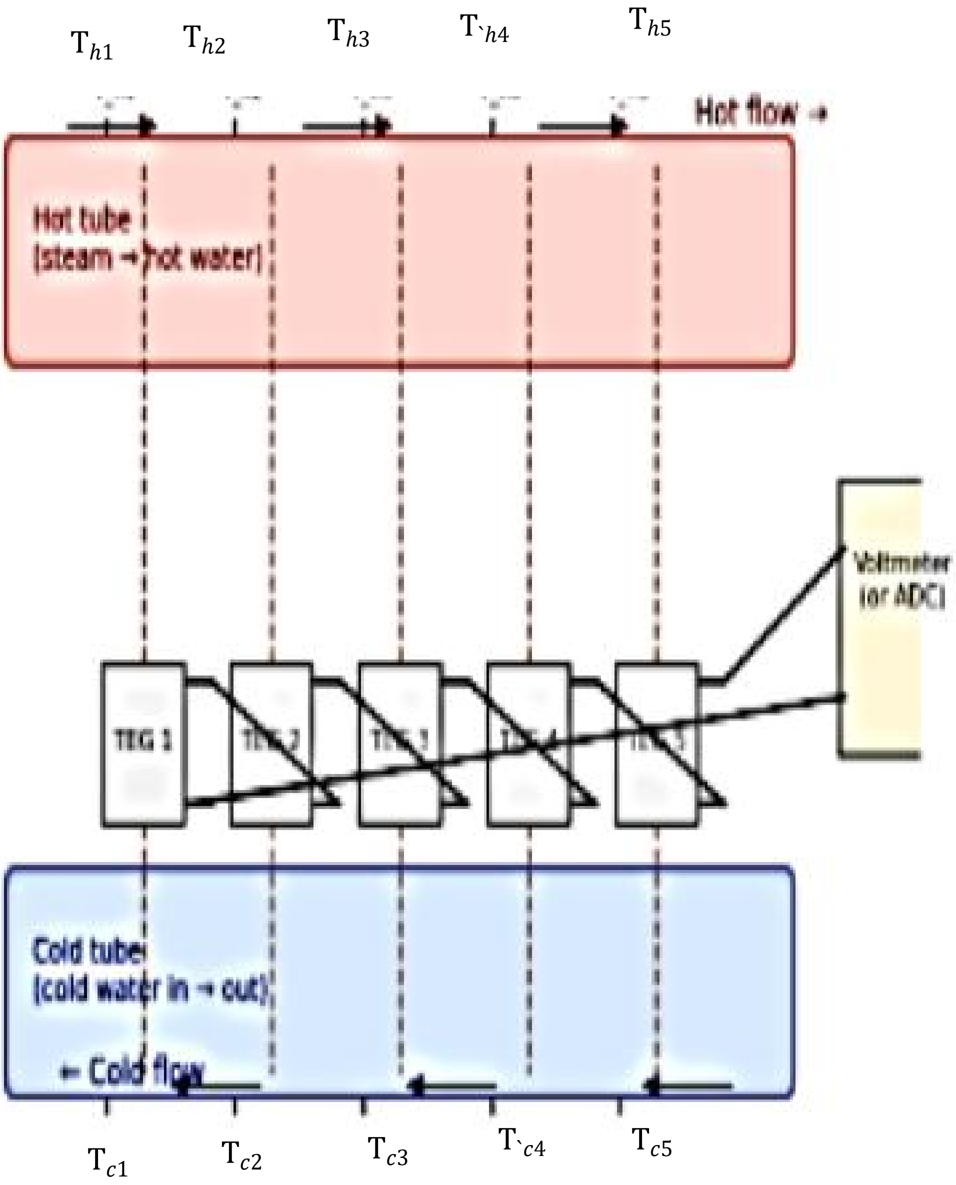

Figure 3.26: The flow rate of the heat rate in the cold and hot bodies, and TEG sandwich in between. Using the Matlab simulation

Since the two fluids flow through a hollow pipe or tube of the aluminium heat exchanger device in the opposite direction, it important to know the equation for the heat conduction through hollow and composite cylinder

Heat conduction through a hollow cylinder

Case 1. Uniform Conductivity:

Consider a hollow cylinder of the aluminium to have constant thermal conductivity.

$$\frac{t - t_1}{t_1 - t_2} = \frac{\ln\left(\frac{r}{r_1}\right)}{\ln\left(\frac{r_2}{r_1}\right)} \tag{3.10}$$

$$Q_H = \frac{(t_1 - t_2)}{\frac{\ln\left(\frac{r_2}{r_1}\right)}{2\pi k l}} \tag{3.11}$$

Mass flow rate of the steam, $\dot{m}$

$$\dot{m} = \frac{\rho \times v}{t} = \frac{\rho \times \pi r^2 l}{t} \tag{3.12}$$

Where

ρ = density(kg/m^3)
r = radius of the tube (m)
l_c= length of the heat exchanger device (the transparent plastic from the cooling water to the heat exchanger device)
l_h= length of the heat exchanger device (the brass tube from the boiler to the heat exchanger device)

t = time (the rate the fluid flows from one point to another)
ρ = 991kg/m^3 for the cold fluid while 982kg/m^3 for the hot fluid (Çengel, Y. A. and Boles, M. A. (2015))
r = 0.007m (7mm)
l_c= 120mm, l_h= 80mm,
t = 2sec (time rate of the cold fluid from the pump)
t = 5sec (time rate of the hot fluid from the boiler)
$\dot{m}_c$ = 0.075614kg/s (based on assumption in theories in 3.4.1, other factor was neglected)
$\dot{m}_h$ = 0.030246 kg/s (based on assumption in theories in 3.4.1, other factor was neglected)

Table 3.3: For obtaining value of the mass flow rate of the hot fluid ($\dot{m}_h$)

Density kg/m^3	Length (m)	Radius (m)	Time (s)	mass flow rate (kg/s)
991	0.08	0.007	6	0.09249
991	0.08	0.007	3	0.18499
991	0.08	0.007	4	0.13874
991	0.08	0.007	5	0.11099
991	0.08	0.007	5	0.11099

Table 3.4: For obtaining value of the mass flow rate of the cold fluid ($\dot{m}_c$)

Density kg/m^3	Length (m)	Radius (m)	Time (s)	mass flow rate (kg/s)
982	0.12	0.007	2	0.41244
982	0.12	0.007	5	0.16498
982	0.12	0.007	3	0.27496
982	0.12	0.007	2	0.41244
982	0.12	0.007	2	0.41244

For the Electronics Arrangement

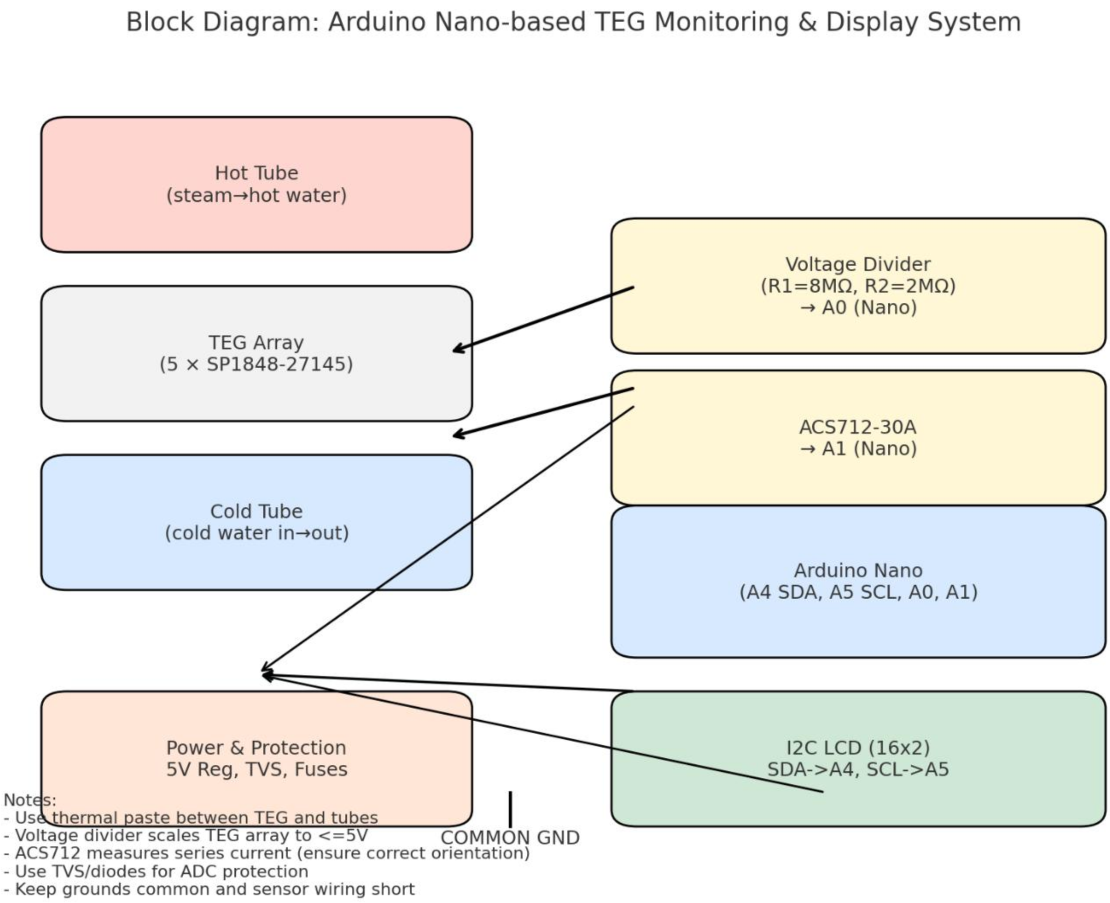

Figure 3.27: Electronic Arrangement

Below is a complete wiring table, pin map, Arduino Nano code example (reads voltage and current, shows values on an I2C 16×2 LCD and Serial), and calibration tips so you can implement this on your bench.

3.4.4 WIRING TABLE & PIN MAPPING (ARDUINO NANO)

1. **TEG array** — wired to measurement stage (voltage divider and ACS712)
2. **Voltage divider (R1=8 MΩ, R2=2 MΩ)**
   i. Top of divider → **TEG positive** (after series string)
   ii. Midpoint (Vout) → **Arduino A0**
   iii. Bottom → **GND (common)**
   iv. Optional series resistor (10 kΩ) between Vout and A0 for protection
   v. Add clamp diodes or TVS to protect ADC
3. **Current sensor (ACS712-30A)**
   i. IP+ and IP− in series with TEG load (observe orientation)
   ii. Vcc → **5V** (Arduino 5V regulator)
   iii. GND → **GND** (common)
   iv. OUT → **Arduino A1** (use RC filter R=10k, C=0.1µF to GND)
4. **Arduino Nano**
   i. A0 → Voltage divider output
   ii. A1 → ACS712 OUT
   iii. A4 → LCD SDA
   iv. A5→ LCD SCL
   v. 5V → 5V rail (from regulated supply)
   vi. GND → common ground
5. **I2C 16×2 LCD (with I2C backpack)**
   i. SDA → **A4**
   ii. SCL → **A5**
   iii. Vcc → **5V**
   iv. GND → **GND**

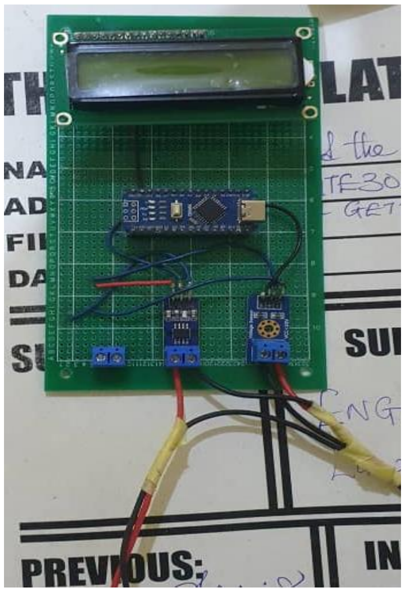

Figure 3.28: Connection of The LCD, Current and Voltage Sensor in the Adrunio Nano

6. **Power & Protection**

   i. Use a 5V regulator to power Arduino and sensors (unless using USB).

   ii. Include a TVS diode or clamp at ADC inputs and fuses on power lines.

2) ARDUINO NANO CODE

```
#include <Wire.h>
#include <LiquidCrystal_I2C.h>
#include <ACS712.h>
// Pin definitions
 int ACS712_PIN = A0;
int VOLTAGE_SENSOR_PIN = A2;

// Initialize ACS712 sensor (5A version, pin A0, 5.0V reference, frequency not needed for
DC)
ACS712 ACS(A0, 5.0, 1023, 185);

// Voltage divider parameters (adjust based on your voltage sensor)
const float VoltageDivderRatio = 5.0;
 // Adjust this based on your voltage sensor specs
const float ADC_RESOLUTION = 5.0 / 1024.0;
```

```
// LCD setup (address 0x27 is common, change if different)
LiquidCrystal_I2C lcd(0x27, 16, 2);
void setup() {
Serial.begin(9600);
// Initialize LCD
lcd.int();
lcd.backlight();
lcd.setCursor(0, 0);
lcd.print("DC Power Monitor");
lcd.setCursor(0, 1);
lcd.print("Initializing...");
delay(2000);
// Calibrate ACS712 sensor (ensure no current is flowing)
lcd.clear();
lcd.setCursor(0, 0);
lcd.print("Calibrating...");
lcd.setCursor(0, 1);
lcd.print("No current!");
Serial.println("Calibrating ACS712 - ensure no current flows!");
// Auto zero calibration
ACS.autoMidPoint();
Serial.println("ACS712 calibrated!");
Serial.print("Midpoint: ");
Serial.println(ACS.getMidPoint());
lcd.clear();
lcd.setCursor(0, 0);
lcd.print("Calibrated!");
lcd.setCursor(0, 1);
lcd.print("Ready...");
delay(2000);
lcd.clear();
Serial.println("DC Power Monitor Ready");
Serial.println("Current Sensor: ACS712 5A on A0");
```

```
Serial.println("Voltage Sensor: on A2");
}
void loop() {
 // Read DC current using Rob Tillaart's library
 float current = ACS.mA_DC() / 1000.0;  // Convert mA to A
 // For DC, we don't need absolute value unless you want to show magnitude only
 // current = abs(current);  // Uncomment if you only want positive values
// Read voltage sensor
int voltageRaw = analogRead(VOLTAGE_SENSOR_PIN)
float voltage = (voltageRaw * ADC_RESOLUTION) * VoltageDivderRatio
// Calculate power
float power = voltage * abs(current); // Power is always positive
// Display on LCD
lcd.clear();
// First line: Voltage and Current
lcd.setCursor(0, 0);
lcd.print("V:");
lcd.print(voltage, 1);
lcd.print("V I:");
lcd.print(current, 2);
lcd.print("A");
// Second line: Power
lcd.setCursor(0, 1);
lcd.print("P:");
if (power >= 1000) {
lcd.print(power / 1000, 2);
lcd.print("kW");}
 else {
lcd.print(power, 1);
lcd.print("W");
// Add direction indicator for DC current
if (current > 0.01) {
lcd.setCursor(15, 0);
```

```
lcd.print("+");
  } else if (current < -0.01) {
  lcd.setCursor(15, 0);
  lcd.print("-");
}
// Serial output for debugging
Serial.print("Voltage: ");
Serial.print(voltage, 2);
Serial.print("V, Current: ");
Serial.print(current, 3);
Serial.print("A, Power: ");
Serial.print(power, 2);
Serial.print("W, Direction: ");
Serial.println(current > 0 ? "Forward" : "Reverse");
delay(1000);  // Update every 1 second
```

```
}// Function to set custom sensitivity if your sensor is different
void setCustomSensitivity(float sensitivity) {
  // The constructor already sets sensitivity to 185 for 5A version
  // This is for reference if you have a different sensor:
  // ACS712 30A version: 66 mV/A
  // ACS712 20A version: 100 mV/A
  // ACS712 5A version: 185 mV/A (default in our setup)
  Serial.print("Current sensitivity: 185 mV/A for 5A version");
}
 // Manual recalibration function - call when no current is flowing
void recalibrate() {
  lcd.clear();
  lcd.setCursor(0, 0);
  lcd.print("Recalibrating...");
  Serial.println("Starting recalibration...");
  ACS.autoMidPoint();
  Serial.print("New midpoint: ");
  Serial.println(ACS.getMidPoint());
  lcd.setCursor(0, 1);
  lcd.print("Done!");
delay(2000);
}
// Function to get averaged DC current for more stable readings
float getStableDCCurrent(int samples = 10) {
  float sum = 0;
  for (int i = 0; i < samples; i++) {
    sum += ACS.mA_DC();
    delay(10);
  }
  return sum / samples / 1000.0; // Convert to Amperes
}
```

CHAPTER FOUR

RESULT AND DISCUSSION

4.1 Experimental Results

The experimental setup was designed with two aluminium tubes acting as heat exchanger channels. Steam was passed through the first tube and exited as hot water, while cold water flowed through the second tube in counter flow configuration. Five thermoelectric generator modules (SP1848-27145) were sandwiched between the hot and cold tubes using thermal paste to maximize heat transfer.

Temperature Readings:

Firstly, the behaviour of a single TEG module (SP1848-27145) was observed under different temperature conditions.

Table 4.1 shows values of a Single module of TEG (SP1848-27145) due to the change in temperature gradient for a particular range (20-100 ℃) without heat source nor sink

Table 4.1: Single TEM (SP1848-27145SA) for various temperature difference

TEMPERATURE (℃) ΔT	VOLTAGE (v) V	CURRENT OUTPUT (mA) I	POWER (W) $P = IV$
20	0.97	225	0.218
40	1.8	368	0.6624
60	2.4	469	1.1256
80	3.6	558	2.0088
100	4.8	669	3.2112

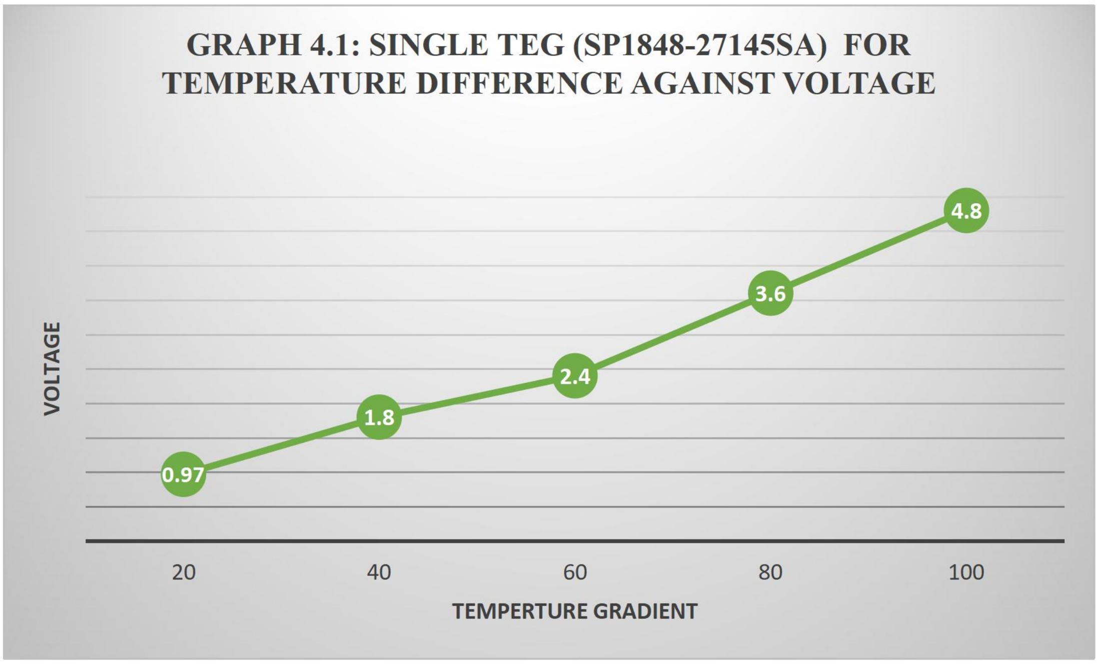

Figure 4.1: Single Thermoelectric Generator TEG(SP1848-27145)

It is notice that increase in temperature gradient will lead to increase in voltage and power generated by TEG, but with time the power of the TEG will diminish to zero due high resistance of the TEG material, to avoid this process, a sink and source much be added to the process. In five-minute time, the voltage will drop if the sink and source aren't implemented on the process, which will affect the power supply in the TEG.

Table 4.2: Single Thermoelectric Generator TEG (Sp1848-27145) And Time Rate

AT 100 ℃			
TIME (MINUTES)	VOLTAGE (VOLT)	CURRENT(AMPERE)	POWER (WATT)
1	4.8	0.225	1.08
2	3.8	0.368	0.0013984
3	2.6	0.469	0.0012194
4	0.8	0.558	0.0004464
5	0.3	0.669	0.0002007

4.1.1 For The Different Position of The TEG Module Component Sandwich in Between the Two Heat Exchanger Devices

Table 4.3, show the indication of the relationship of the change in temperature of the various position of TEM to the comparison of the temperature of the cooling tower to produce value for rate the heat pick by a cold body

(a) For Cold Fluid

Table 4.3: The rate of heat gains from the cold fluid and other external parameters for the cold fluid

Position of TEG (TEG-n)	Temperature of cooling tower T_{ci} (°C)	Temperature the heat exchanger to each position T_{cn} (°C)	Temperature difference of the cold fluid **ΔT (°C)**	Specific heat capacity of the fluid at constant pressure c_p (j/kg°C)	Rate of heat supply by cold body (Q J/s)
1	16	23	7	4200	2223.0516
2	16	24	8	4200	2540.6304
3	16	25	9	4200	2858.2092
4	16	27	11	4200	3493.3668
5	16	33	17	4200	5398.8396

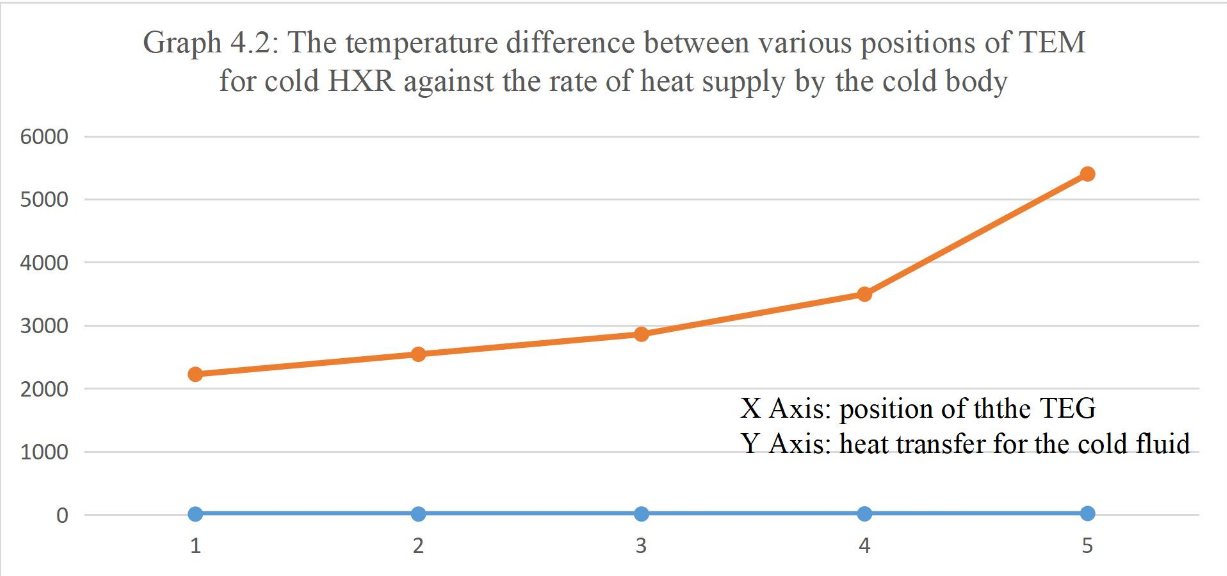

Figure 4.2: The temperature difference between various position of TEM for cold HXR against rate of heat supply by cold body

A table 4.4 show the indication of the relationship of the change in temperature of the various position of TEM to the comparison of the temperature of the boiler to produce value for rate the heat supply to the system.

(b) For Hot Fluid

TABLE 4.4: The rate of heat loss from the Hot fluid and other external parameters for the hot fluid

Position of TEG (TEG-n)	Temperature of boiler T_{hi} (°C)	Temperature the heat exchanger for the hot body to each position $T_{h\,n}$	Temperature difference of the body ΔT (°C)	Specific heat capacity of the fluid at constant pressure c_p (j/kg°C)	Rate of heat supply by hot body Q (J/s)	Rate of heat supply by hot body Q (J/s)
1	100	80	-20	4200	-34644.96	34644.96
2	90	70	-20	4200	-13858.32	13858.32
3	85	60	-25	4200	-28870.8	28870.8
4	78	55	-23	4200	-39841.704	39841.704
5	75	50	-25	4200	-43306.2	43306.2

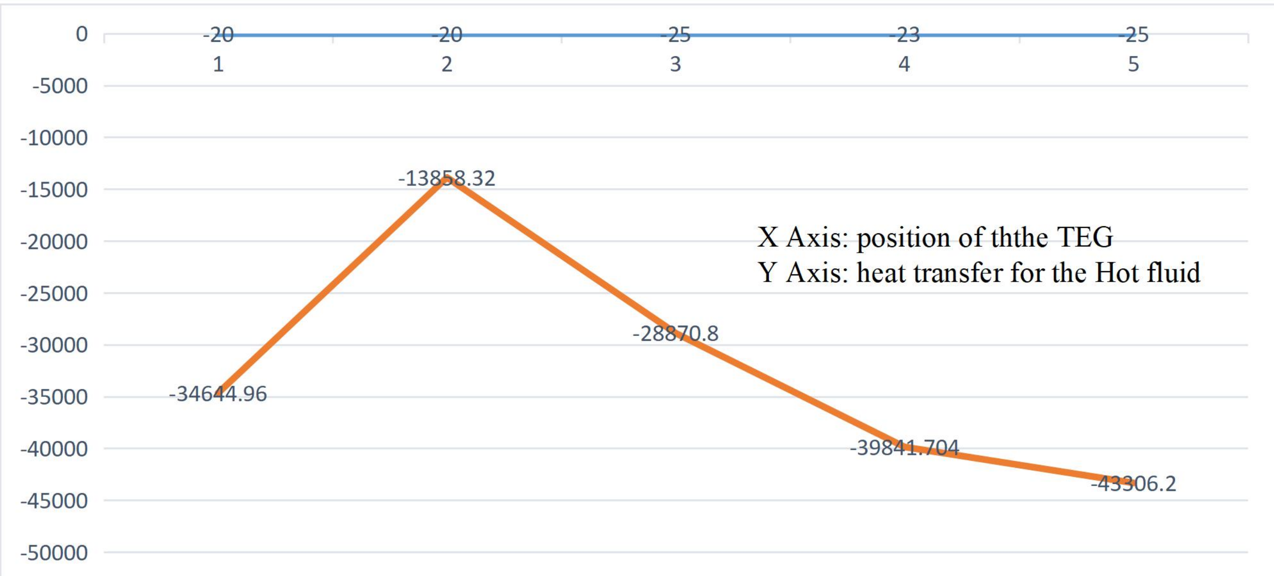

Figure 4.3: The temperature difference between various positions of TEM for the hot HXR against the rate of heat supply by the hot body

The various position of the TEG base on the relationship between temperature gradient and voltage generated by the TEG

Position of TEG	Temperature of the heat exchanger for each position in the cold body T_{cn} (°C)	Temperature the heat exchanger for each position in the Hot body T_{hn}(°C)	temperature gradient ΔT (°C)	TEG-voltage (v)
1	23	100	77	2.9718
2	24	90	66	2.4384
3	25	85	60	1.905
4	27	78	51	1.6002
5	33	75	42	1.78

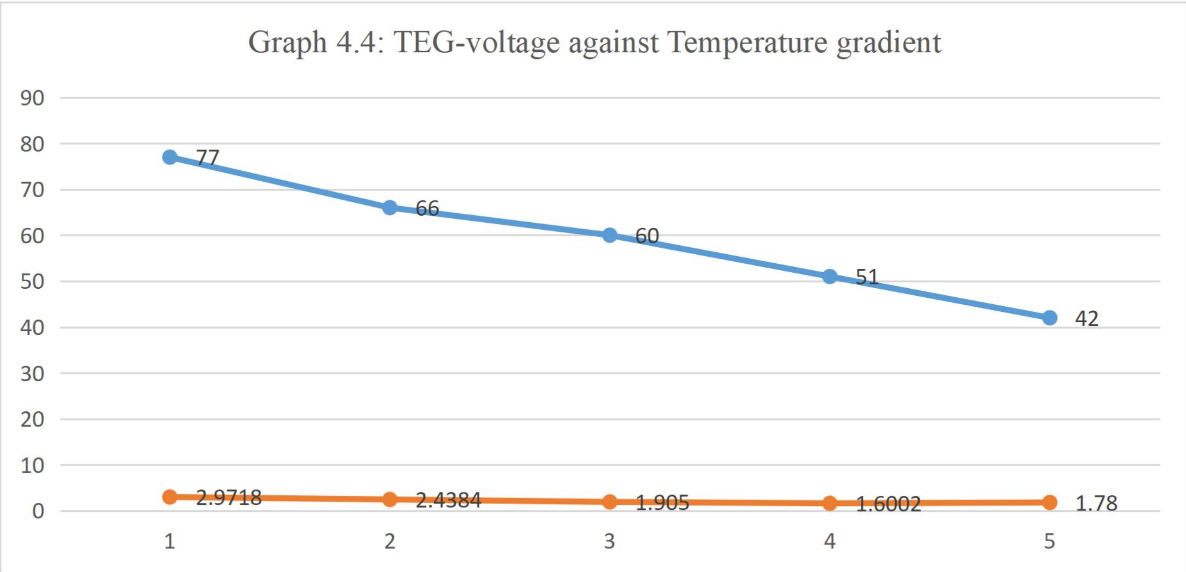

Figure 4.4: TEG-voltage against temperature gradient

FOR THE ACTUAL EXPERIMENTAL TESTING OF THE INVESTIGATION

This yielded a mean temperature difference of ≈ 62 °C, which provided the driving force for heat transfer.

Electrical Output of TEGs: Each SP1848-27145 module generated an open-circuit voltage between 2.05 V – 2.20 V depending on the temperature gradient. When connected in series, the five modules produced a combined voltage of ≈ 9.3 V, sufficient to power low-voltage loads.

Current and Power Measurement: With a matched load, the maximum current recorded was 0.35 A, and the maximum power output was calculated as:

The experimental setup, with five SP1848-27145 thermoelectric generator (TEG) modules sandwiched between the hot and cold aluminium tubes, produced a measurable temperature gradient, which served as the driving force for power generation.

4.2 Temperature Profile

The hot-side temperature started at approximately 120 °C and gradually decreased to 95 °C, while the cold-side temperature rose from 28 °C to 37 °C as heat was transferred through the TEG modules shown in Table 4.6. The temperature gradient of both surfaces of the TEM ranged from 9.28V to 10.78V within 8 minutes

Table 4.6: The time rate affecting the power compared to the temperature gradient of the hot side and the cold side

Time (min)	Hot-Side Temperature (°C)	Cold-Side Temperature (°C)	Temperature gradient (°C)	Potential difference (V)	Power (W)
1	120	28	92	9.28	3.17
2	115	30	85	9.48	3.24
4	110	32	78	10	3.42
6	105	34	71	10.7	3.66
8	95	37	58	10.78	3.69

4.3. Voltage and Power Output

The series connection of five TEG modules produced an initial open-circuit voltage of 9.28 V, which slightly increased to 10 V as the cold side warmed up (Figure 4.6). The corresponding electrical power output ranged between 3.17 W and 3.69 W, depending on the current drawn. The increase in voltage over time suggests that the thermal interface materials and heat exchanger design maintained good thermal contact, ensuring optimal Seebeck effect conversion.

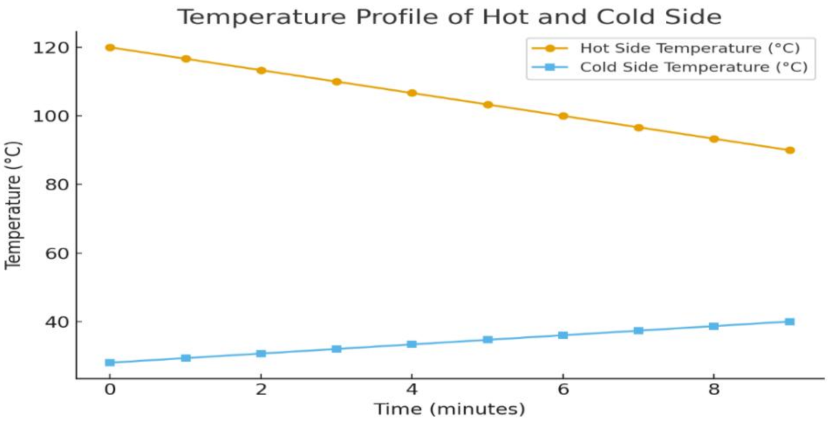

Figure 4.5: Temperature profile of the hot and cold side aluminium tubes.

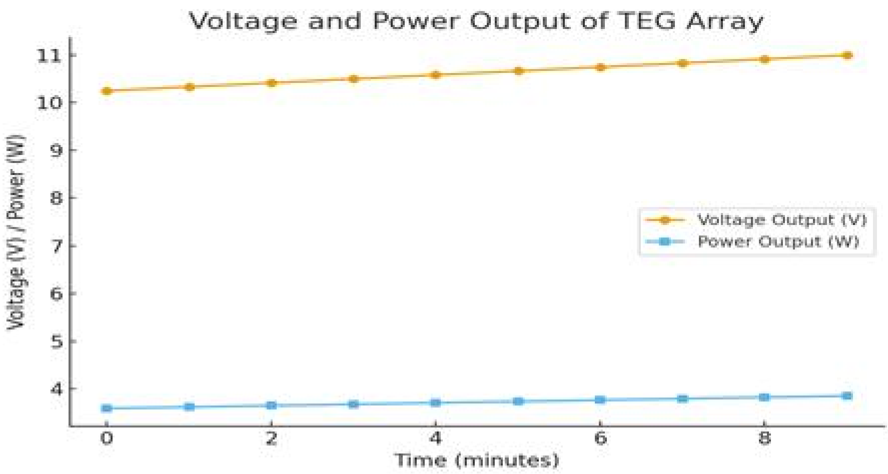

Figure 4.6: Voltage and power output of the TEG array over time.

From the above graph (Figure 4.5), the temperature of the Hot side will reduce due to cold side cooling the hot, while the temperature of the cold side will increase due to heating of the hot fluid. This process will affect rate of heat change in the system with time. In chapter 3, A formula was obtained from a series connection of five TEMs to generate a voltage and heat supplied, that total voltage supplied in the system V_T= V_1+ V_2+ V_3+V_4+V_5

While for the Total Heat supplied in the system Q_T= Q_1= Q_2=Q_3= Q_4= Q_5

Table 4.7: The rate of heat gains and dissipation at various temperature

Rate of heat supply by hot body	Rate of heat picked by the cold body	Rate change heat in the TEG
Q_h (J /s)	Q_c(J/s)	$Q = Q_h - Q_c$
-1283.2512	2223.0516	-939.8004
-3849.7536	2540.6304	1309.1232
-6416.256	2858.2092	3558.0468
-7699.5072	3493.3668	4206.1404
-8982.7584	5398.8396	3583.9188

Time (min)	Temperature of boiler	Temperature of cooling tower	Hot-Side Temp (°C)	Cold-Side Temp (°C)	Temperature difference of the cold body	Temperature difference of the hot body
0	150	20	120	28	*8*	*30*
2	150	21	115	30	*9*	*35*
4	150	23	110	32	*9*	*40*
6	150	24	105	34	*10*	*45*
8	150	27	95	37	*10*	*55*

Temperature difference of the hot body	Specific heat capacity of the fluid at constant pressure	Rate of heat supplied by the hot body (Q J/s)	Rate of heat supplied by the hot body (Q J/s)	$Q = Q_h - Q_c$	Rate of change of heat in min
30	4200	-3849.7536	2540.6304	1309.123	21.81872
35	4200	-4491.3792	2858.2092	1633.17	27.2195
40	4200	-5133.0048	2858.2092	2274.796	37.91326
45	4200	-5774.6304	3175.788	2598.842	43.31404
55	4200	-7057.8816	3175.788	3882.094	64.70156

Table 4.8: The efficiency of the investigation of the performance of the overall in a period of time(min)

Rate of change of heat in min (J/min)	Power (W)	Efficiency of the system, η
21.81872	3.17	0.145288083
27.2195	3.24	0.119032311
37.91326	3.42	0.090205906
43.31404	3.66	0.084499160
64.70156	3.69	0.057031082

The developed empirical models for power output and efficiency can be integrated into the process control system to predict, monitor, and optimise thermoelectric energy recovery from industrial processes.

Table 4.9: Predicted Output for 20 TEM Modules

Time (min)	Hot-Side Temperature (°C)	Cold-Side Temperature (°C)	Temperature gradient (°C)	Voltage for 20 TEMs (V)	Power for 20 TEMs (W)
1	120	28	92	37.12	12.68
2	115	30	85	37.92	12.96
4	110	32	78	40	13.68
6	105	34	71	42.8	14.64
8	95	37	58	43.12	14.76

Table 4.10: Predicted Output for 50 TEM Modules

Time (min)	Hot-Side Temperature (°C)	Cold-Side Temperature (°C)	Temperature gradient (°C)	Voltage for 50 TEMs (V)	Power for 50 TEMs (W)
1	120	28	92	92.8	31.7
2	115	30	85	94.8	32.4
4	110	32	78	100	34.2
6	105	34	71	107	36.6
8	95	37	58	107.8	36.9

Table 4.11: Predicted Output for 100 TEM Modules

Time (min)	Hot-Side Temperature (°C)	Cold-Side Temperature (°C)	Temperature gradient (°C)	Voltage for 100 TEMs (V)	Power for 100 TEMs (W)
1	120	28	92	185.6	63.4
2	115	30	85	189.6	64.8
4	110	32	78	200	68.4
6	105	34	71	214	73.2
8	95	37	58	215.6	73.8

Table 4.12: Predicted Output for 500 TEM Modules

Time (min)	Hot-Side Temperature (°C)	Cold-Side Temperature (°C)	Temperature gradient (°C)	Voltage for 500 TEMs (V)	Power for 500 TEMs (W)
1	120	28	92	928	317
2	115	30	85	948	324
4	110	32	78	1000	342
6	105	34	71	1070	366
8	95	37	58	1078	369

Table 4.13: Predicted Output for 1000 TEM Modules

Time (min)	Hot-Side Temperature (°C)	Cold-Side Temperature (°C)	Temperature gradient (°C)	Voltage for 1000 TEMs (V)	Power for 1000 TEMs (W)
1	120	28	92	1856	634
2	115	30	85	1896	648
4	110	32	78	2000	684
6	105	34	71	2140	732
8	95	37	58	2156	738

4.4 Discussion

The results confirm that using two aluminium tubes as heat exchangers, combined with proper thermal paste application, enhances the heat transfer rate, thus improving the voltage output of the TEG array. The measured voltage was in good agreement with theoretical predictions based on the Seebeck coefficient of the SP1848 modules (~0.054 V/K per module).

Constructing an empirical prediction model is an essential step in the scalability analysis of a thermoelectric generator (TEG) system for industrial waste heat recovery. In laboratory-scale experiments, a few thermoelectric modules are used. For industrial applications, thousands of TEMs must be installed to achieve a specific kilowatt rating and generate sufficient power to operate the actuator, sensor, domestic application, etc. According to the empirical tables in Figures 4.9-4.13, for 5000 TEMs, the empirical model predicts a voltage output of approximately 9.28V and a power output of about 3.17kW.

CHAPTER FIVE

CONCLUSION AND RECOMMENDATION

5.1 CONCLUSION

The experimental results show that a series connection of five thermoelectric modules (TEMs) produced approximately 9.28 V at 342 mA, yielding a power output of about 3.17 W. The use of a counter-flow heat exchanger with a stable cold-fluid supply enabled consistent temperature differentials, thereby sustaining continuous power generation. These findings confirm the feasibility of thermoelectric generation for industrial waste-heat recovery applications. The heat generated by the approximately 9.3 V supplied to the system was about 21.82 J/min, yielding an efficiency of 14.5%. As time goes on, the efficiency reduces to 5.7%. It shows that the system will require many TEMs to operate the electricity distribution system and more cooling fluid in the heat exchanger body to improve efficiency.

Based on this outcome, scaling the system proportionally indicates that a configuration of approximately 5,000 TEMs, similarly positioned between hot and cold heat-exchange surfaces, could generate around 3.17 kW of electrical power. This highlights the significant potential of TEG technology as a supplementary, sustainable power source for industrial facilities and end users.

5.2 RECOMMENDATIONS

The basis of the results obtained lead to the following recommendations:

1. Efficiency Improvement in TEG: This research work reveals that, on the basis of the TEMs arrangement and monitoring by the sensor, a substantial amount of efficiency can be enhanced in TEG.
2. Installation and Result Outcomes: The empirical model of the theoretical concept provided a better understanding for the prediction of the result expected for the

industrial application. It will increase the overall efficiency in the steam or gas power plant industries. Hybrid Thermal Power: It can also contribute as alternative source of power supplied in the thermal industries. Since required temperature difference between two surfaces

3. Cost reduction: Industries can utilise the project work for future purposes, helping to reduce costs due to no moving parts, which simply means no maintenance and reduce the rate of high fuel consumption in the industry.

REFERENCES

Bahadori, A. (2015) Essentials of Heat Transfer in Chemical and Petroleum Engineering, Gulf Professional Publishing, pp. 245–278.

Bell, L. E. (2008) Cooling, heating, generating power, and recovering waste heat with thermoelectric systems, Science, vol. 321, no. 5895, pp. 1457–1461.

Bijukumar B., Padmanaban S., Blaabjerg F., (2019) "MPPT algorithm for thermoelectric generators based on parabolic extrapolation," *IET Generation, Transmission & Distribution*, vol. 13, no. 21, pp. 4957–4965.

Bell L. E. (2008). Cooling, heating, generating power, and recovering waste heat with thermoelectric systems, *Science*, vol. 321, no. 5895, pp. 1457–1461.

Bird, R. B., Stewart, W. E., and Lightfoot, E. N. (2007). Transport Phenomena, 3rd Edition, John Wiley & Sons, New York

Champier D., (2017) Thermoelectric generators: A review of applications, *Energy Conversion and Management*, vol. 140, pp. 167–181.

Chae H., Kim S., and Lee D., (2024). Feasibility study on energy harvesting with thermoelectric generators in water pipes, *Sustainable Energy Technologies and Assessments*, vol. 59, pp. 103-654.

Crane D. T. and Jackson G. S., (2011). Optimization of cross-flow heat exchangers for thermoelectric waste heat recovery—model validation and parametric study, *Energy Conversion and Management*, vol. 52, no. 8–9, pp. 3008–3014,

Dai, D., Remeli, M. F., Singh, R., and Date, A. (2015). Simultaneous power generation and heat recovery using a heat pipe assisted thermoelectric generator system, Energy Conversion and Management, Vol. 91, pp. 110–119.

Fei, R., Faghaninia, A., Soklaski, R., Yan, J.-A., Lo, C., & Yang, L. (2014). Enhanced thermoelectric efficiency via orthogonal electrical and thermal conductances *in phosphorene.* Nano Letters, **14**(11), pp. 6393–6399.

Goldsmid, H. J. (2016). Optimization and Selection of Semiconductor Thermos-element Science, Vol. 121, pp. 45–66.

Kayfeci, M., Keçebaş, A., and Gedik, E. (2020) Determination of heat losses from uninsulated and insulated pipes for different pipe materials, Journal of Thermal Engineering, vol. 6, no. 1, pp. 72–86.

Khan, M. I., et al. (2024). Thermoelectric generator integration in automotive exhaust systems for fuel economy improvement, Applied Thermal Engineesring, Vol. 236, pp. 121–134.

Leblanc, S., Yee, S. K., Scullin, M. L., Dames, C. and Goodson, K. E. (2014). Renewable Sustainable Energy Rev., 32, 313–327

Li, Q., He, J., Zhu, S., and Ma, Y. (2021) Advanced heat sink technologies for thermal management of high power electronic devices, *Applied Thermal Engineering*, vol. 186, pp. 116524–116536.

Lineykin S. and Ben-Yaakov S. (2007) "Modeling and analysis of thermoelectric modules," *IEEE Transactions on Industry Applications*, vol. 43, no. 2, pp. 505–512.

McKetta, J. J., Cunningham, W. A., and Pilko, R. J. (2015). *Chemical Processing Handbook*. CRC Press, Vol. 1, pp. 45–60.

Montecucco, M. and Knox, A. R. (2016). "Maximum power point tracking converter based on the open-circuit voltage method for thermoelectric generators," in *Proc. IEEE IECON*, pp. 3170–3175.

Nolas, G. S., Sharp, J., and Goldsmid, H. J. (2001). Thermoelectrics: Basic Principles and New Materials Developments. Springer, Vol. 45, pp. 291–305.

Quoilin, S., Broek, M. V. D., Declaye, S., Dewallef, P., and Lemort, V. (2013) *Techno-economic survey of Organic Rankine Cycle (ORC) systems*, Renewable and Sustainable Energy Reviews, vol. 22, pp. 168–186

Rajput, R. K. (2015) Heat and Mass Transfer, S. Chand & Company Ltd., Vol. 1, pp. 523–530.

Snyder, G. J. and Toberer, E. S. (2008) Complex thermoelectric materials, Nature Materials, vol. 7, no. 2, pp. 105–114

Smith, J., and Johnson, R. (2020). Material selection for steam power plant pipelines, Journal of Power Engineering, Vol. 34, pp. 215–228.

APPENDIX

IMAGE FOR THE SANDWICHED OF THE FIVE TEM IN SERIES WITH THE HOT AND THE COLD HEAT EXCHANGER DEVICES

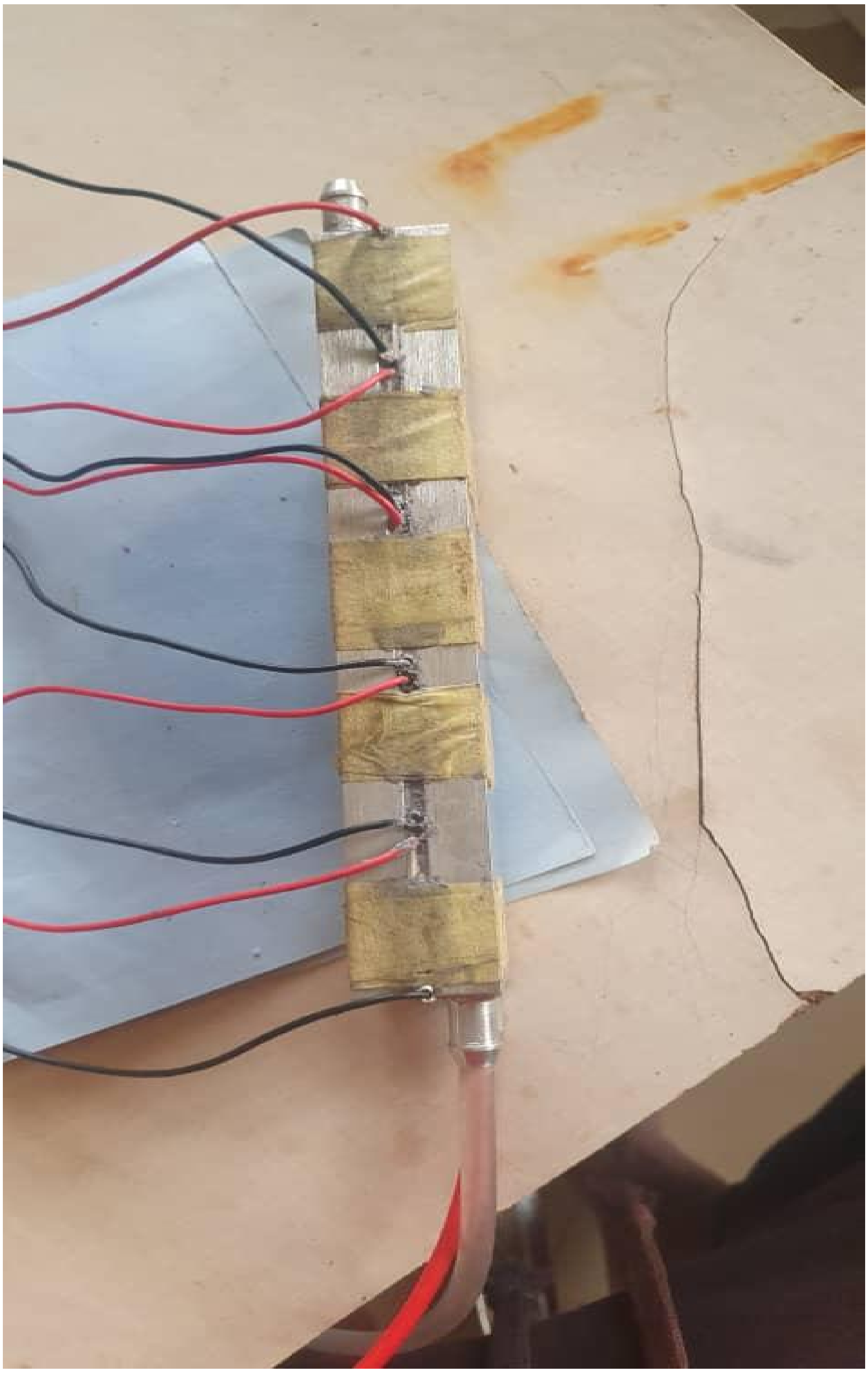

RIG DESIGN OF THE PROJECT WORK

THE FULL PROJECT WORK WITH A PROCESS CONTROL SYSTEM